Beyond 5G White Paper
6G Radio Technology Project
“Sensing Technologies”

Version 1.0

May 7, 2025

XG Mobile Promotion Forum

XGMF

【Revision History】

Ver.	Date	Contents	Note
1.0	2025.05.07	Initial version	

Preface

In our published white paper "Beyond 5G White Paper ~Message to the 2030s~", we researched what are required in various industries in the Beyond 5G/6G era, then we proposed "Further enhancement of specific 5G features" as key features for Beyond 5G/6G. To address these key features, Target Key Performance Indicators (Target KPI) for Beyond 5G/6G have been derived, and as quantitative Target KPI related with "Sensing", sensing accuracy/resolution with order of centimeter (and more) has been introduced, which is much higher than that with order of meters in 5G.

The Third Generation Partnership Project (3GPP) has initiated discussions on Integrated Sensing and Communication (ISAC) for the secondary use of radio waves. Defined use cases include the detection of human and animal intrusions in indoor/outdoor environments and understanding the status of automobiles and automatic guided vehicles. Sensing technologies utilizing radio waves have found widespread applications in detecting the distance and direction of objects, among other functionalities. With the current rapid advancements in Artificial Intelligence (AI) and Machine Learning (ML), their application scope continues to broaden, particularly in shape, motion, and gesture detections.

Sensing technologies can be considered in both aspects of Beyond 5G/6G advancement through sensing as well as sensing with Beyond 5G/6G. First, let us consider the sensing for Beyond 5G/6G. Sensing of wireless environments in Beyond 5G/6G mobile communications is performed while transmitting data, and making this sensing more accurate is essential for improving performances of the wireless communications. The sensing data obtained here can be used not only for the wireless communications, but also for various applications as mentioned above. Next, let us consider Beyond 5G/6G for the sensing. The use of high-frequency radios including millimeter-wave and terahertz bands is also expected to realize high-precision spatial sensing and localization (including positioning) by taking advantage of their properties. Such sensing is provided by the wireless communications (fixed and movable base stations) and optical communications. A basic principle of wireless sensing is to characterize the status and behavior of a target object as radio propagation characteristics in wireless channels; a Received Signal Strength Indicator (RSSI) and Channel State Information (CSI) are useful as feature information for the wireless sensing. CSI-based sensing is crucial for integrating communication and radar sensing. Many studies have shown its adaptability for various sensing tasks. However, the CSI-based sensing faces an open issue: how information in physical space (sensing environment) is reflected in CSI observations. To address this, further research is needed to better understand the relationship between the physical space and the CSI observations.

In addition to such wireless sensing, network architecture to collect and process large amounts of data from cameras, Light Detection And Ranging (LIDAR), and other sensors, as well as sensing of the physical space as a digital twin are also expected.

However, there are still major challenges in the practical implementations for the design and evaluation of ISAC as a core technology in the Beyond 5G/6G system. First and foremost, a theoretical framework is necessary to analyze and evaluate the performance of current ISAC solutions to identify the benefits and any short comings. Current design of the ISAC system calls for the baseband and RF hardware to be functionally shared and as a trade-off, the impact of distortion parameters on sensing performance needs to be carefully considered. The challenge for the joint waveform design is the very different KPIs for communication and sensing where optimizing both might not be so straight forward.

ISAC in the mobile communication network provides great opportunities and benefits for synchronized multi-static sensing where the technology challenges here would lie in the synchronization to achieve the optimum fusion sensing results. Concretely, current Global Navigation Satellite System (GNSS) fails to provide pico-second level synchronization accuracy to base stations, and new space-time synchronization should be provided with that level of accuracy, enabling the phase-locked synchronization in the millimeter wave between the base stations.

To tackle these challenges and realize new use cases, there are a lot of research and development activities on the sensing technologies in Japan. As 6G Radio Technology Project of XGMF, this white paper summarizes both technical overview of ISAC and recent Japanese research and development (R&D) activities on the sensing technologies in the 6G radio technology field, including the content of Beyond 5G White Paper Supplementary Volume "Sensing Technologies" already published by XGMF. Specifically, this white paper introduces in detail cutting-edge R&D efforts on the sensing technologies in Japan as follows:

- “CSI-Based Device-Free Sensing Using Deep Learning with 5G NR 28 GHz Band” describes an overview of device-free sensing technology, which detects target object without the need for mobile terminals, utilizing deep learning. It further introduces the effectiveness of this technology by experiments using a radio testbed equipped with the physical layer specifications of the 28 GHz-band 5G NR.

- “Indoor Experimental Evaluation of Device-free Localization Schemes Using Channel State Information in Distributed Antenna Systems” describes a real-time CSI-based device-free localization scheme for distributed antenna systems, where CSI feedback frames are collected and used as a dataset for ML-based localization. Experimental results confirm that the localization scheme is effective for detecting a target in an indoor environment.

- “CSI2Image: CSI-to-Image Conversion using a Generative Model” describes how to convert CSI observations into RGB images corresponding to physical space using generative adversarial network (GAN) architecture. The generated RGB images intuitively show the relationship between the CSI observations and the physical space and potentially help us to extract many environmental parameters for multi-purpose sensing system.

- "Use Cases for CSI Sensing with an Example of Pedestrian Movement Direction Identification" describes use cases for CSI sensing from the perspectives of commercial products and the author's research, and specifically the effectiveness of pedestrian movement direction identification as one of the use cases for CSI sensing is verified by experimental evaluation with ML.

- "Integrated Sensing and Communication (ISAC)" describes a concept of ISAC, typical use cases, and two case studies of how to use ISAC to improve localization accuracy and perform millimeter-level imaging at the THz band using future portable devices. The research challenges to implementing ISAC in practice are discussed.

- "Space-Time Synchronization" describes that synchronization must not only be limited to time but also extend to space, entailing the sharing (synchronization) of spatial coordinate axes. The space-time synchronization is realized by three basic technologies, namely compact atomic clocks, wireless time synchronization, and cluster clock systems, which are explained briefly.

- "Experimental Evaluation of WLAN-based Device-Free Localization Using CSI in Outdoor and Large-scale Indoor Environments" describes that the developed localization scheme enhances the localization accuracy in specific areas effectively by properly positioning the access point (AP) and the terminal. And also the research discusses the degree to which performance difference is observed in various scenarios with different AP and terminal positions.

- "A Fundamental Study on the Relationship Between Pedestrian Traffic and Wi-Fi CSI with Existing Outdoor Access Points" describes the relationship between pedestrian traffic and Wi-Fi CSI with existing outdoor APs. The results show a correlation between CSI variation and congestion conditions, demonstrating the feasibility of estimating pedestrian traffic using CSI variation from existing Wi-Fi APs.

- "Multipath-RTI: Millimeter-Wave Radio Based Device-Free Localization" describes Multipath-RTI, a novel radio tomographic imaging (RTI) method utilizing millimeter-wave (mmWave) signals for device-free localization (DFL). The study introduces compressed sensing-based image reconstruction, automatic parameter tuning, and DBSCAN clustering for multi-target location estimation. Results from simulations and mmWave channel sounding measurements show sub-0.5 m accuracy in complex indoor environments.

- "Verification in an Anechoic Chamber toward the Realization of a Radio Wave Camera Using a Mobile Communication System" describes that the 5GNR downlink signal reflected from a target is received by a virtual array antenna, and the reference signal demodulation and direction estimation algorithms are applied in order to perform sensing without significantly disrupting the frame format of 3GPP-compliant signals. This result shows that it is possible to estimate the direction of a target by utilizing the reference signal contained in the 5GNR downlink signal.

In conclusion, as we embark on the journey towards Beyond 5G/6G, the sensing technologies emerge as one of key elements in this technological evolution. Japan's endeavor to overcome the challenges to realize the sensing technologies, coupled with its commitment to research and development in this domain, positions it at the forefront of this next-generation mobile communication revolution. This white paper aims to provide a comprehensive overview of the potential, challenges, and future directions of the sensing technologies for Beyond 5G/6G, with a particular emphasis on their initiatives and advancements in Japan.

This white paper was prepared with the generous support of many people who participated in Wireless Sensing Working Group of 6G Radio Technology Project, XGMF. The cooperation of telecommunications industry players as well as academia experts has also been substantial. Thanks to everyone's participation and support, this white paper was able to cover a lot of useful information for future discussions on business creation between industry, academia, and government, and for investigating solutions to social issues, not only in the telecommunications industry, but also across all industries. We hope that this white paper will help Japan create a better future for society and promote significant global activities.

Satoshi Suyama

NTT DOCOMO, INC.

Tomoki Murakami

NTT Corporation

I. Technical Overview of Integrated Sensing and Communications (ISAC)

Shuhei Saito
Panasonic Holdings Corporation
Hideya So
Kogakuin University of Technology & Engineering
Tomoki Murakami
NTT Corporation
Nobuaki Kuno, Takahiro Tomie, Koshiro Kitao, Satoshi Suyama
NTT DOCOMO, INC.

I-1. Introduction

In the fifth-generation-advanced (5G-A) and sixth-generation (6G) systems, new intelligent applications and services, such as autonomous driving and extended reality (XR), are expected to be realized. Such applications require both high-data-rate transmission and high-resolution sensing [1]. However, due to the shortage of spectrum resources, it is difficult to satisfy the spectrum requirements to support 5G-A and 6G. Accordingly, integrated sensing and communication (ISAC), which unifies the functions of wireless communications and radar sensing, has been gaining increasing attention [1], [2]. In the ISAC systems, the functions of communications and radar share the same frequency band and hardware equipment, thereby improving the spectrum efficiency, reducing the device's size, and saving energy consumption.

To facilitate new mobile applications in 5G-A and 6G systems, the International Mobile Telecommunications (IMT)-2030 aims to support ISAC as usage scenarios, such as activity detection and movement tracking, environmental monitoring, and provision of sensing data on surroundings for artificial intelligence (AI), XR, and digital twin applications [3]. These applications must fulfill the following requirements: high-precision positioning, range/velocity/angle estimation, and imaging.

On the other hand, ISAC faces several challenges in achieving high performances in communication and radar. From the communications perspective, ISAC applications require combating interference and channel fading. The radar function requires good autocorrelation, combating large Doppler frequency shifts, and massive signal bandwidth and dynamic range [1]. Moreover, ISAC systems must perform high accuracy within low complexity and limited computation resources.

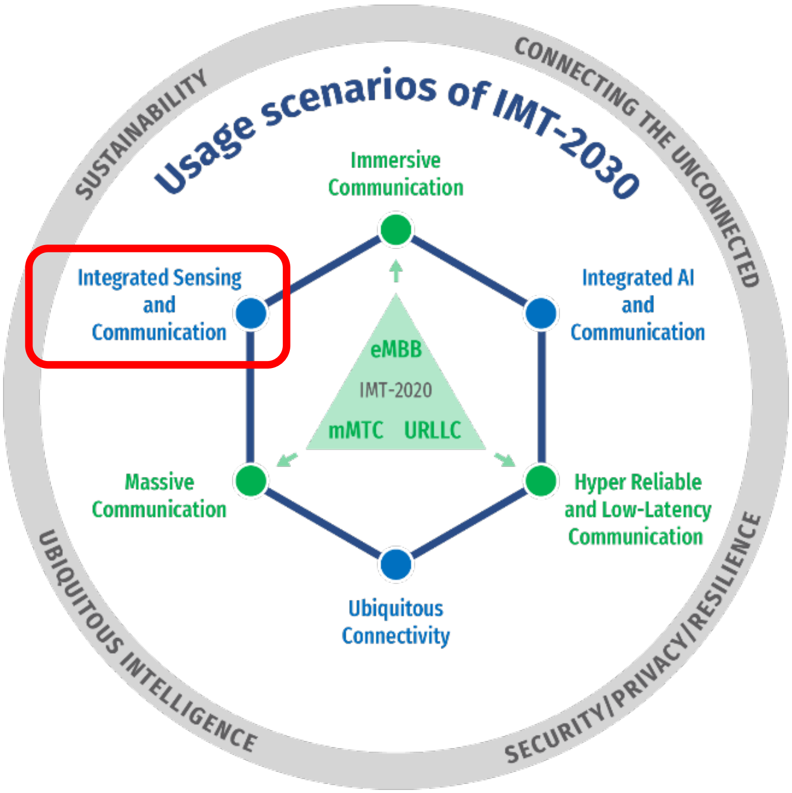

Figure II-1.1 Usage scenarios of IMT-2030 [3].

I-2. Objective for standardization in 3GPP

In response to the growing momentum of ISAC applications and the vision presented in IMT-2030, the standardization of ISAC specifications has also begun within the 3rd Generation Partnership Project (3GPP) [4]. Although 3GPP supposes the radio access technology (RAT)-based positioning, however, the current specifications do not offer the in-built capability to detect objects not connected to the network: The existing channel models in the technical report (TR) 38.901 [5] do not address target modelling, sensing, background environment modelling, and differentiation from targets. Therefore, it is important to establish a solid channel modelling framework to enable the evaluation of sensing techniques for such use cases mentioned above.

Considering these backgrounds, 3GPP has identified a wide range of use cases for ISAC applications in TR 22.837 [6]. Moreover, 3GPP sets three objectives in the study item (SI) [4]: (1) channel modelling, (2) sensing modes, and (3) frequency.

(1) Channel modelling: One of the goals is to define channel modelling aspects to support object detection and/or tracking. The technical specification (TS) 22.137 [7] aims at a common modelling framework capable of detecting and/or tracking the following example objects (sensing targets) and enabling them to be distinguished from unintended objects:

a. Uncrewed aerial vehicles (UAVs),
b. Humans indoors and outdoors,
c. Automotive vehicles (at least outdoors),
d. Automated guided vehicles (AGVs, e.g., in indoor factories), and
e. Objects creating hazards on roads/railways, with a minimum size dependent on frequency.

(2) Sensing modes: This study defines six sensing modes, as shown in Figure II-2.1.

(3) Frequency: Frequencies from 0.5 to 52.6 GHz are the primary focus, with the assumption that the modelling approach should scale to 100 GHz (If significant problems are identified with scaling above 52.6 GHz, the range above 52.6 GHz can be deprioritized).

Accordingly, 3GPP aims to identify the details of the deployment scenarios corresponding to the above use cases. In particular, this study aims to define the channel modelling details for sensing based on the conventional specification TR 38.901 as a starting point and take into account relevant measurements, including:

a. Modelling of sensing targets and background environment, including radar cross-section (RCS), mobility, and clutter/scattering patterns,
b. Spatial consistency.

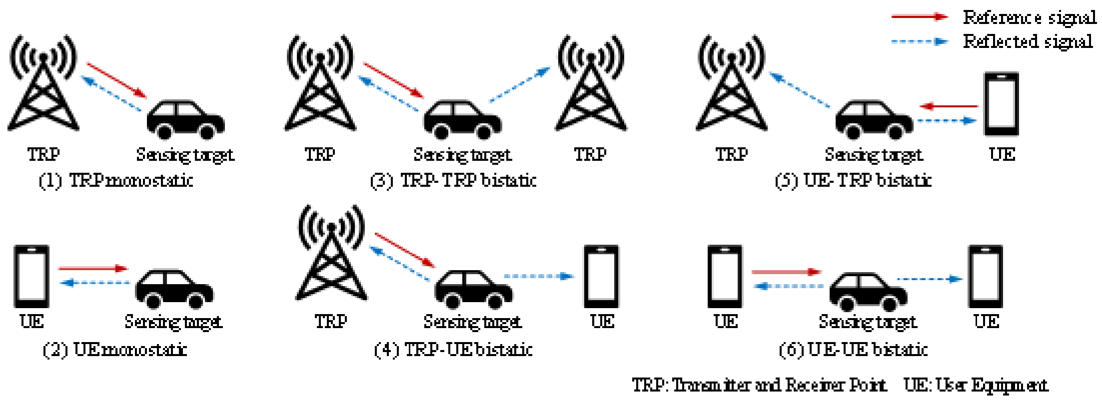

Figure II-2.1 Sensing modes of ISAC.

I-3. Use case in 3GPP

In TR 22.837 [6], a study item on ISAC was agreed to study channel modeling and deployment scenarios to detect and/or track the following example objects (sensing targets), as shown in Table II-3.1.

Table II-3.1 Use cases classifications based on sensing targets [6].

(1) UAVs ● UAV flight trajectory tracing ● Network-assisted sensing to avoid UAV collision ● Sensing for UAV intrusion detection ● UAVs, vehicles, and pedestrian detection near Smart Grid equipment	**(2) Humans indoors and outdoors** ● Intruder detection in smart home ● Contactless sleep monitoring service ● Health monitoring at home ● Service continuity of unobtrusive health monitoring ● Roaming for sensing service of sports monitoring ● Immersive experience based on sensing ● Use case public safety search and rescue or apprehend
(3) Automotive vehicles (at least outdoors) ● Sensing-assisted automotive maneuvering and navigation ● Sensing for parking space determination ● Vehicles sensing for ADAS ● Sensing for automotive maneuvering and navigation service when not served by RAN ● Blind spot detection	**(4) Automated guided vehicles (AGVs, e.g., in indoor factories)** ● AGV detection and tracking in factories ● Autonomous mobile robot (AMR) collision avoidance in smart factories
(5) Objects crating hazards on roads/ railways, within a minimum size dependent on frequency ● Pedestrian/animal intrusion detection on a highway ● Sensing for railway intrusion detection ● Sensing at a crossroads with/without obstacle ● Accurate sensing for automotive maneuvering and navigation service	**(6) Combination of (1)~(5). and other targets** ● Rainfall monitoring ● Transparent sensing use case ● Sensing for flooding in smart cities ● Intruder detection in surroundings of smart home ● Sensing for tourist spot traffic management ● Protection of sensing information ● Sensor groups ● Seamless XR streaming ● Coarse gesture recognition for application navigation and immersive interaction

Figure II-3.1(a) shows an example of detecting UAV intrusion over flight routes. Many low-altitude UAVs will be used in smart cities for complex and diverse tasks. However, the dense deployment of UAVs makes supervision difficult if only the traditional radar systems are used. Moreover, non-cooperative UAVs intruding in some no-fly zones (e.g., airports and military bases) would lead to serious consequences, such as exposing private information using the camera and blocking other UAV traffic on the flying route. Therefore, the 5G system can detect UAV intrusion in restricted areas.

Figure II-3.1(b) shows an example of health monitoring in an elderly house. The deployed 5G system installed in a hospital or elderly home includes multiple sensing devices, which can perform health monitoring, such as fall/activity detection of vital signs (e.g., heart rate or breathing rate), and wireless sensing of vital signs. Installing cameras has privacy concerns, whereas sensing devices have the advantage that there is no need to recharge/replace the batteries of body-worn sensors and remind/help residents to wear them after they take them off.

Figure II-3.1(c) shows an example of parking space determination using the ISAC system. As shown in Figure II-3.1(c), sensing technology can improve the user experience in the parking garage by sharing information. Connectivity is an important component in automatic parking, such as automated valet parking (AVP) and automatic factory parking (AFP). 3GPP sensing technology can serve as a way to determine available parking spaces and the best route for a car to reach them.

Figure II-3.1(d) shows a concept of collision avoidance in smart factories. Autonomous mobile robots (AMRs) can travel automatically without guides using the central unit that conducts scheduling, routing, and dispatching decisions. However, due to the AMR's sensing range limitation, the surrounding environment status may not be detected in time. 5G base stations deployed in a factory can provide communication capabilities for equipment in the factory and sense the surrounding environment. Therefore, sensing results can be utilized to improve the efficiency and driving safety of AMRs.

Figure II-3.1(e) shows a concept of sensing at crossroads. Traffic accidents often happen at the crossroads, for example, owing to the sudden appearance of pedestrians from an invisible place. Thus, there is an urgent need to monitor the real-time road status. With the collaboration of trusted third parties, such as map service providers or management platforms of intelligent transport systems (ITS), driving warnings or assistant driving information can be provided timely to vehicles. The cameras and radars on roadside units (RSUs) have some blind points, whereas 5G-based sensing can provide sensing information to fill these gaps.

Figure II-3.1(f) shows an example of flood detection in smart cities. Due to the rapid climate change in recent years, it can be challenging to predict where flooding occurs using cameras and other sensors. Instead of these devices, sensing employing radio waves can efficiently alternate flood detection.

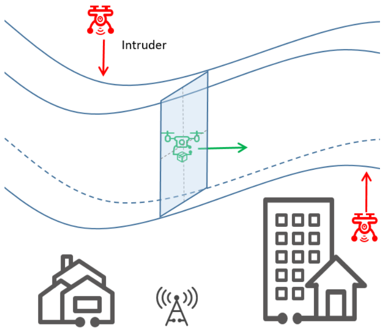

(a) Detection of UAV intrusion

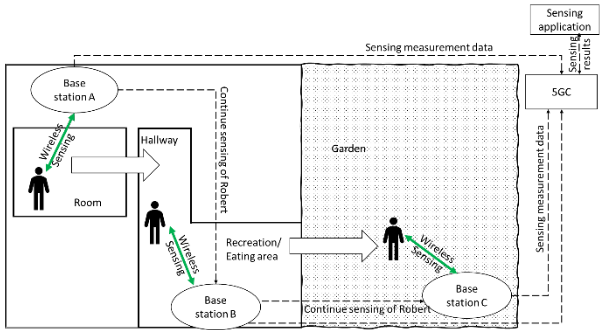

(b) Health monitoring in elderly house

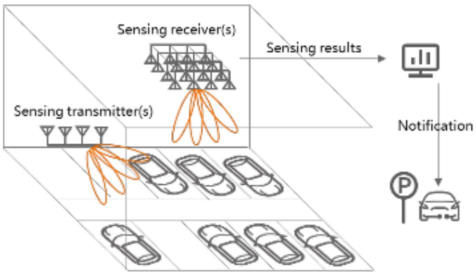

(c) Parking space determination

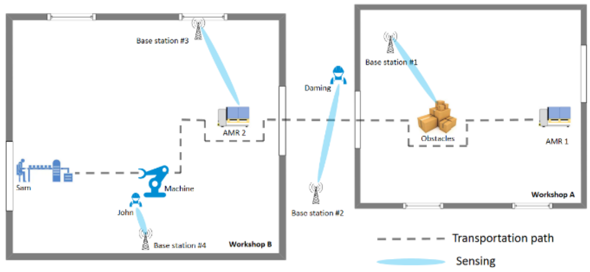

(d) Collision avoidance in smart factories

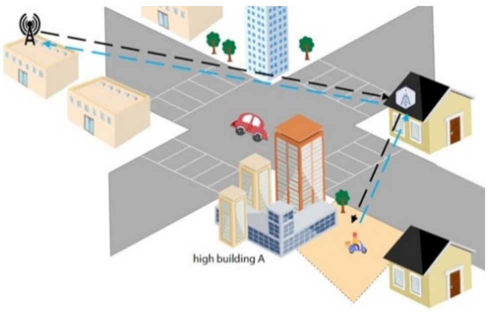

(e) Sensing at crossroads

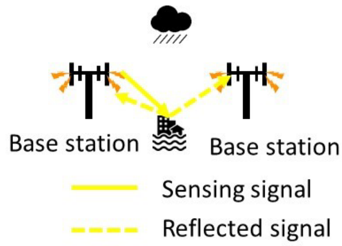

(f) Detection of flood

Figure II-3.1 Examples of the ISAC scenarios [6].

I-4. Progress of ISAC in 3GPP

Figure II-4.1 shows an example of a roadmap for 3GPP ISAC standardization provided by a 3GPP delegate [8]. As shown in Figure II-4.1, the initial discussion of ISAC in 5G-A Release 19 (Rel-19) began in 2024. In the 3GPP service aspect (SA), the feasibility study on ISAC as a SI [6] and the service requirements for ISAC as a work item (WI) [4] have been completed. In the 3GPP radio access network (RAN), the simulation parameters of each ISAC sensing target have been agreed upon. Currently, discussions on the channel modelling for ISAC are ongoing. Until the middle of 2025, discussions will focus on the ISAC channel modelling for 5G-A [8], [9]. In particular, the specifications for the commercial and industrial use of UAVs are prioritized owing to the rapid growth in the business and industrial demands [8]-[10]. On the other hand, a lot of open issues remain as follows [11]:

(1) ISAC deployment scenarios

- Remaining issues on channel model calibration/evaluation parameters
- Calibration of the ISAC channel model

(2) ISAC channel modelling

a. Physical object modelling

- Collection of values for RCS model of UAV, human, vehicle, and AGV
- Polarization matrix of target
- Details on modelling objects with multiple scattering points
- Correlation of RCS in adjacent incident and scattered angles
- Forward RCS

b. Channel model

- Remaining details of the basic ISAC channel model
- Background channel for monostatic sensing mode
- Exact sections in the existing TR as a reference to generate
- Target channel modelling for targets with multiple scattering points
- Remaining details on environment object (EO) type-2
- Details on power normalization combining target channel and background channel
- Absolute time of arrival
- Forward scattering and blockage

c. **Further details on spatial consistency**

- Which links should spatial consistency apply, Tx-target link, target-Rx link, and Tx-Rx link (i.e., background channel) of the same or different Tx/target/Rx
- Site-specific or target-specific correlation parameters, including 3D spatial consistency
- Consideration of EO

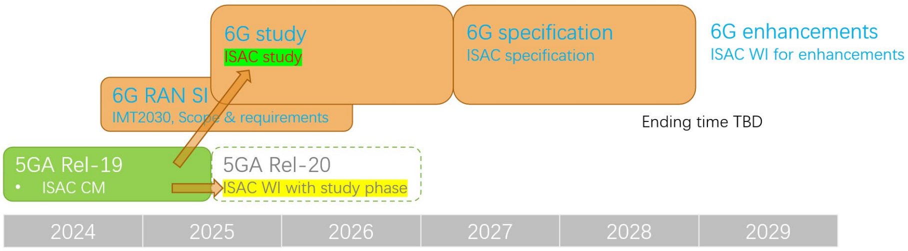

Figure II-4.1 An example of a roadmap for 3GPP ISAC standardization [8].

I-5. Channel model

The discussion of ISAC channel modeling started from the March 2024 RAN1 meeting by agreement on the following formula [12], [13].

$$H_{ISAC} = H_{target} + H_{background}$$

In addition to this formula, it is based on a common framework as shown in Figure II-5.1. It was first agreed that the ISAC channel model should consist of two channels: a target channel influenced by the sensing target and a background channel unaffected by the target. In addition to the target, for example, an object that is different from the target but knows its location is defined as environment object (EO), and the discussion started based on how to determine the details of each channel of the target, background, and EO. Furthermore, environmental objects are classified into EO type-1 if they are the size and shape equivalent to the sensing target (For example, people, UAV, AGV etc.), and EO type-2 if they are much larger than the target (For example, walls, buildings, grounds, etc.), and the effects of each type will be discussed in detail [13].

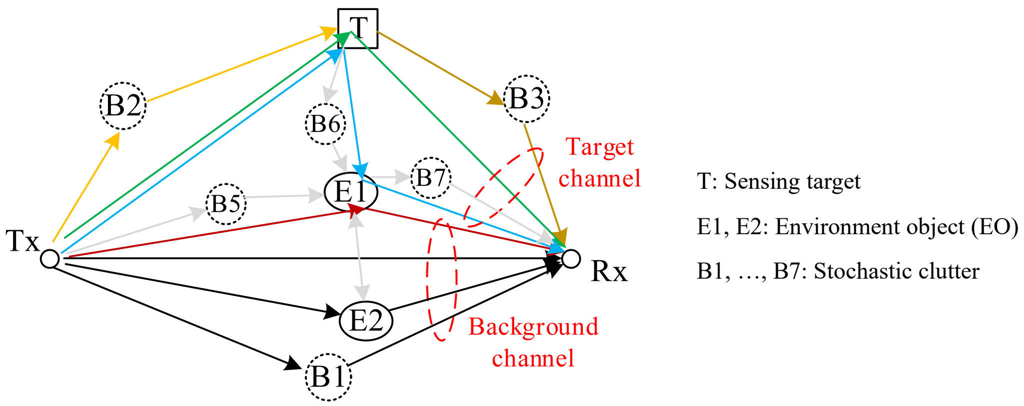

Figure II-5.1 The common framework for ISAC channel model [13][14].

The basis such as the generation of stochastic clusters by the target channel, and the deterministic parameters at the TRP and target were started by using the existing model of TR38.901 [15]. And it was agreed that the scattering point in the target is divided into single case and multiple case, and that the sensing is mainly by the value of RCS (radar reflection cross section) in the single scattering point [16], [17]. Figure II-5.2 shows an example of the discussion on the target RCS value in monostatic sensing [16]. In addition to discussing the RCS model for each target, the remaining issues such as target polarization, diffraction/blockade modeling, multi-scattering point target modeling, EO type-2 modeling, and spatial consistency modeling are being discussed at the recent meeting [18], [19].

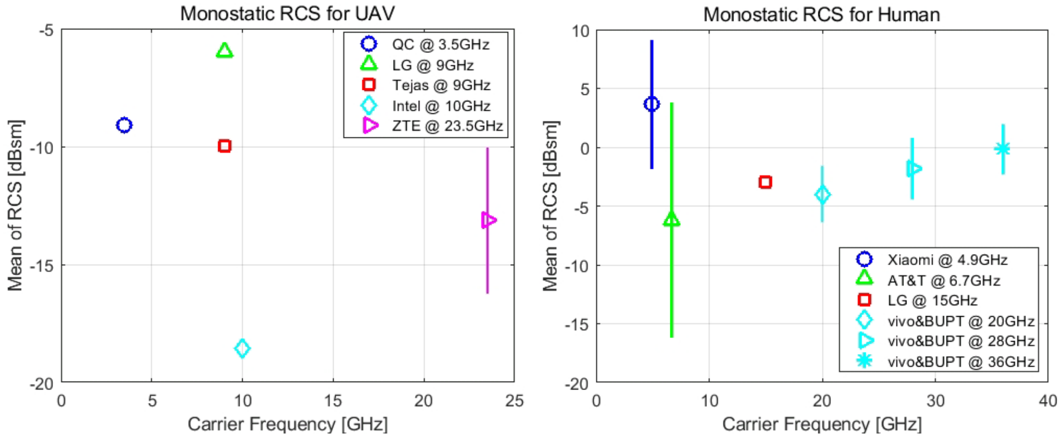

Figure II-5.2 An example of the discussion on the target RCS value.

I-6. Technology trend

I-6.1. Categories of Sensing methods

The general categories of sensing methods are depicted in Figure II-6.1.1. Sensing can first be classified into two types: active sensors, which generate signals from the device itself, and passive sensors, which receive signals emitted by the environment. In ISAC, research has predominantly focused on active sensors; however, depending on the frequency used for sensing, the application of passive sensors may also be considered. Active sensors include sensing methods that utilize radar or communication signals. Radar-based sensing transmits specialized radar signals, such as pulse signals or Frequency Modulated Continuous Wave (FMCW) signals and detects parameters such as distance and Doppler shift based on the changes in these signals. This enables the detection of distance and objects and has led to the practical implementation of systems such as collision detection and weather radar. In contrast, communication-based sensing involves utilizing communication signals either in their original form or with partial extensions for sensing purposes. By integrating these methods into existing communication systems, sensing can be performed while minimizing capital investment and power consumption. The modulation schemes used include single carrier and multi-carrier, with ongoing research and development on specific modulation techniques for sensing applications. Among these, a new modulation scheme known as Orthogonal Time Frequency Space (OTFS) is being investigated, with promising future prospects. A key challenge in ISAC lies in how to effectively integrate these categories into communication systems, while constructing a comprehensive system that includes considerations of sensing accuracy.

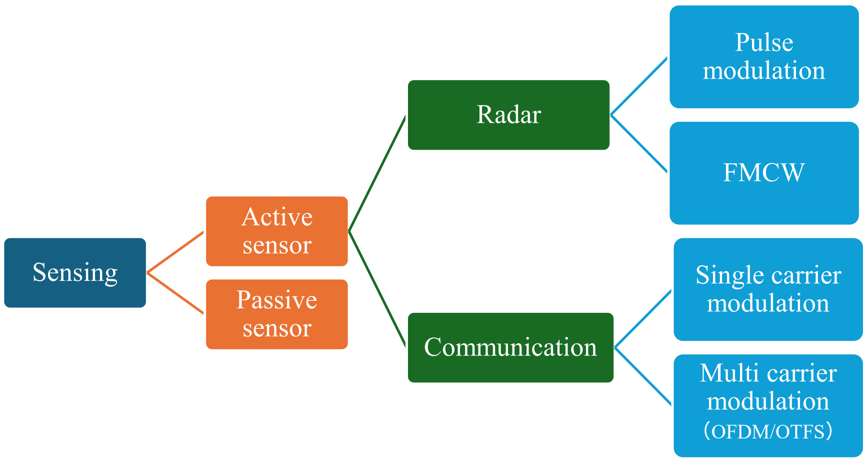

Figure II-6.1.1 Categories of sensing methods.

I-6.2. Publication Summary

Table II-6.2.1 presents a summary of a survey on ISAC-related papers that will be registered in IEEE Xplore. As shown in the Table II-6.2.1, the classification is based on the use cases defined by 3GPP. Specifically, the results are categorized into Outdoor use cases, including Human, Animal, Vehicle, UAV, and Weather, as well as Indoor use cases. It should be noted that, although there are existing papers on Wi-Fi in the context of sensing technologies, these are excluded from this analysis. Furthermore, papers that include experimental studies are highlighted in gray and papers that include this white paper's articles are highlighted in yellow. The results indicate that ISAC has been primarily studied for use cases other than Animal.

Sensing using Wi-Fi signals is also being explored. This includes detecting the presence of humans and objects, detecting actions such as falls and walking, and detecting and tracking the location of humans and objects. Both scenarios, where the target to be detected has a Wi-Fi device and where it does not, are being considered, and many studies use CSI (Channel State Information) as feedback signals. This is an approach that utilizes the existing Wi-Fi system, making it a sensing technology that leverages the existing specifications. Furthermore, many studies focus on detecting humans and objects indoors. This is likely because Wi-Fi uses an unlicensed band, and using the same frequency as other systems could cause interference, so minimizing this interference is a key concern.

On the other hand, sensing is also being considered for outdoor environments, in addition to indoors. Similarly to indoor sensing using Wi-Fi signals, detection of humans and objects is being explored outdoors. Sensing using millimeter waves in frequency bands is also being studied, offering higher resolution compared to Sub-6, allowing for more precise detection. For example, detection of sleep and respiration is also being performed.

For outdoor sensing, in addition to humans and objects, detection of moving bodies such as vehicles and UAVs is being considered. To ensure safety, it is desirable to be able to track the positions of these moving bodies in real-time. If the moving body carries a device, position estimation can be achieved by measuring the received power. However, in some cases, the moving body may not be able to transmit control information containing its location. Therefore, passive sensing methods such as Time Difference of Arrival (TDOA) and Frequency Difference of Arrival (FDOA) are used to estimate the position. Additionally, methods to extract control information features from the moving body and detect its state from RF signal differences are also being studied.

In addition to objects, weather sensing is also being explored. By analyzing the received power of signals during adverse weather conditions such as rain or snow, the state can be classified, and the weather can be determined. Studies are also being conducted to estimate the probability of rainfall through deep learning. Changes in humidity can also be detected. In such cases, selecting the appropriate frequency band is essential.

Table II-6.2.1 Publication summary of use case in ISAC.

Use case		Publications
Outdoor	Human	[23][25][35][36][37][44][47][48][49][54][55][56][58][59][60]**[II-1][II-4][II-7][II-8][II-10]**
	Animal	
	Vehicle	[20][22][23][26][28][29][30][37][40][41][35][47][48][50][54][55][57]
	UAV	[23][24][32][38][39][43][48][61][62][63][64][65]
	Weather	[66][67][68][69][70][71][72][73][74][75]
Indoor		[21][27][31][33][34][42][46][50][51][52][53][76]**[II-2][II-3][II-9][II-10]**
Other		**[II-5][II-6]**

I-6.3. Publication Trend

Figure II-6.3.1 illustrates trends in the number of publications on ISAC, JSAC/JCAS, and JRC/JCR. The database used to generate this figure consists of journals and conference papers published in IEEE Xplore from 2010 to 2024, with the number of publications containing the following keywords in their titles.

- ISAC: ISAC, integrated sensing and communication
- JSAC/JCAS: JSAC, JCAS, joint communication and sensing , joint sensing and communication
- JRC/JCR: JRC, JCR, joint radar and communication, joint communication and radar

As shown in the Figure II-6.3.1, from 2018 to 2020, the number of publications from JRC/JCR was above a certain level, but from 2021 onwards, the number of publications from ISAC has increased sharply. This is believed to be due to the definitions of terms provided by IMT-2030 and 3GPP. Furthermore, the number of ISAC papers is expected to continue to rise, indicating that it is a field of technology that is gaining attention. On the other hand, the number of publications from JSAC/JCAS and JRC/JCR is also on the rise, but since it is less than one-tenth of the number of ISAC papers, it is clear that conducting a keyword search for ISAC would be sufficient to investigate the technological trends.

Next, a table showing the ranking of technical terms that are used alongside ISAC will be presented. The publication papers used for aggregation are the same as those extracted in Figure II-6.3.1, and the keywords registered for each paper in IEEE Xplore were compiled. By using these keywords, an overview of the current technological trends can be grasped. Words related to use cases are highlighted in green, while words related to technology are highlighted in yellow. In terms of use cases, autonomous driving, UAVs, and object detection, which are being considered for 6G, are ranked highly. In terms of technology, OFDM, MIMO, NOMA, interference full-duplex, and various optimization algorithms are ranked highly.

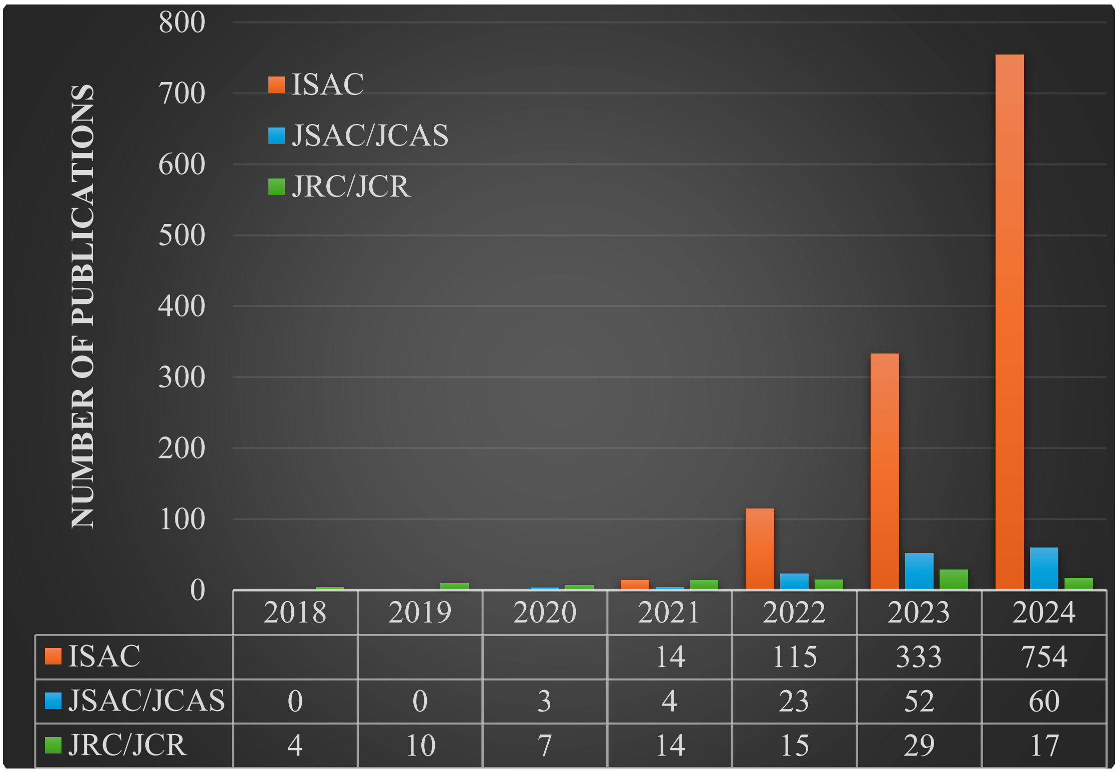

Figure II-6.3.1 Trends in the number of publications in IEEE Xplore.

Table II-6.3.1 Keyword ranking in ISAC publications.

Keyword	Count			
ISAC	800		NOMA	77
sensors	361		deep learning	76
wireless communication	294		signal processing	75
radar	284		real-time systems	75
simulation	274		costs	74
array signal processing	266		bandwidth	68
OFDM	247		beamforming	66
6G	247		precoding	66
optimization	227		signal processing algorithms	66
signal to noise ratio	211		radar tracking	64
receivers	189		antenna arrays	63
interference	185		millimeter wave communication	63
autonomous aerial vehicles	180		channel models	63
estimation	167		quality of service	61
channel estimation	156		training	61
reconfigurable intelligent surfaces	155		transmitting antennas	59
transmitters	142		imaging	58
wireless sensor networks	137		parameter estimation	56
location awareness	131		radio frequency	55
time-frequency analysis	130		throughput	55
conferences	124		performance evaluation	54
symbols	116		heuristic algorithms	54
resource management	113		approximation algorithms	54
base stations	110		delays	52
object detection	102		waveform design	51
spectral efficiency	101		protocols	50
hardware	101		system performance	47
downlink	99		robot sensing systems	47
radar antennas	96		MIMO	46
interference cancellation	92		radar signal processing	46
uplink	89		antenna measurements	44
vehicular and wireless technologies	87		full-duplex system	44
wireless networks	85		physical layer security	43
radar detection	84		target tracking	43
modulation	82		internet of things	43
receiving antennas	79		uav	43
measurement	77			

REFERENCE

[1] A. Liu, Z. Huang, M. Li, Y. Wan, W. Li, and T. X. Han, C. Liu, R. Du, D. K. P. Tan, J. Lu, Y. Shen, F. Colone, and K. Chetty, “A survey on fundamental limits of integrated sensing and communication,” IEEE Communications Surveys & Tutorials, vol. 24, no. 2, pp. 994–1034, Feb. 2022.

[2] Z. Wei, H. Qu, Y. Wang, X. Yuan, H. Wu, Y. Du, K. Han, N. Zhang, and Z. Feng, “Integrated sensing and communication signals toward 5G-A and 6G: A survey,” IEEE Internet of Things Journal, vol. 10, no. 13, pp. 11068–11092, July 2023.

[3] ITU-R Recommendation M.2160-0, “Framework and overall objectives of the future development of IMT for 2030 and beyond,” Nov. 2023.

[4] 3GPP RP-242348, “Revised SID: Study on channel modelling for integrated sensing and communication (ISAC) for NR,” RAN#105, Melbourne, Australia, Sept. 2024. (Revision of RP-240779)

[5] 3GPP TR 38.901 V18.0.0, “Study on channel model for frequencies from 0.5 to 100 GHz (Release 18),” April 2024.

[6] 3GPP TR 22.837 V19.4.0, “Feasibility study on integrated sensing and communication (Release 19),” June 2024.

[7] 3GPP TS 22.137 V19.1.0, “Service requirements for Integrated Sensing and Communication; Stage 1 (Release 19),” Mar. 2024.

[8] 3GPP RP-242803 (Xiaomi), “Views on ISAC in 5GA Rel-20,” RAN #106, Madrid, Spain, Dec. 2024.

[9] 3GPP RP-242863 (China Telecom), “Motivation on integrated sensing and communication for 5G-A Rel-20,” RAN #106, Madrid, Spain, Dec. 2024.

[10] 3GPP RP-243151 (ZTE), “Support of ISAC in 5G-A Rel-20,” RAN #106, Madrid, Spain, Dec. 2024.

[11] 3GPP RP-242804, “Status report for SI: Study on channel modelling for Integrated sensing and Communication (ISAC) for NR,” RAN #106, Madrid, Spain, Dec. 2024.

[12] 3GPP R1-2401937, “Summary #3 on ISAC channel modelling,” TSG RAN WG1 #116, Athens, Greece, March 2024.

[13] 3GPP R1-2403716, “Summary #5 on ISAC channel modelling,” TSG RAN WG1 #116bis, Changsha, China, April 2024.

[14] 3GPP R1-2409908 (Xiaomi, BJTU, BUPT), “Discussion on ISAC channel model,” TSG RAN WG1 #119, Orlando, US, Nov. 2024.

[15] 3GPP R1-2404636, “Summary #4 on ISAC channel modelling,” TSG RAN WG1 #117, Fukuoka, Japan, May 2024.

[16] 3GPP R1-2409280, “Summary #4 on ISAC channel modelling,” TSG RAN WG1 #118bis, Hefei, China, Oct. 2024.

[17] 3GPP R1-2410014, “Summary #4 on ISAC channel modelling,” TSG RAN WG1 #119, Orlando, US, Nov. 2024.

[18] 3GPP R1-241041 (NTT DOCOMO, INC.), “Discussion on ISAC Channel Modelling,” TSG RAN WG1 #119, Orlando, US, Nov. 2024.
[19] 3GPP R1-2501002, “Summary #4 on ISAC channel modelling,” TSG RAN WG1 #120, Athens, Greece, Feb. 2025.
[20] J. Wang, J. Lian and G. Zhu, "A Weighted Mahalanobis Distance Target Sensing Strategy for Underwater Integrated Sensing and Communication Systems," in IEEE Wireless Communications Letters, vol. 13, no. 1, pp. 79-83, Jan. 2024.
[21] Q. Chen, Y. Liang and H. Jiang, "Integrated Sensing And Communication In Unlicensed Mmwave Bands: Joint Beamforming Training And Energy Allocation," ICASSP 2024 - 2024 IEEE International Conference on Acoustics, Speech and Signal Processing (ICASSP), Seoul, Korea, Republic of, 2024, pp. 12926-12930.
[22] Z. Yu and Y. Yang, "Integrated Sensing and Communication Waveform Design for mmWave Vehicular Networks: A Subcarrier Classified Modulation Approach," 2024 IEEE International Workshop on Radio Frequency and Antenna Technologies (iWRF&AT), Shenzhen, China, 2024, pp. 310-314.
[23] D. Singh et al., "A Novel Adaptive Spreading Waveform for Integrated Sensing and Communication," 2024 IEEE 4th International Symposium on Joint Communications & Sensing (JC&S), Leuven, Belgium, 2024, pp. 1-6, doi: 10.1109/JCS61227.2024.10646217.
[24] X. Lu, Z. Wei, R. Xu, L. Wang, B. Lu and J. Piao, "Integrated Sensing and Communication Enabled Multiple Base Stations Cooperative UAV Detection," 2024 IEEE International Conference on Communications Workshops (ICC Workshops), Denver, CO, USA, 2024, pp. 1882-1887, doi: 10.1109/ICCWorkshops59551.2024.10615952.
[25] J. He, L. Yin, J. He, J. Li, S. Xiao and R. Song, "NOMA-LFM Waveform and ANN Scheme for W-Band Integrated Sensing and Communication System," in IEEE Photonics Technology Letters, vol. 36, no. 8, pp. 559-562, 15 April15, 2024, doi: 10.1109/LPT.2024.3379297.
[26] Y. Liu, M. Li, L. Ong and A. Yener, "Bistatic Integrated Sensing and Communication over Memoryless Relay Channels," 2024 IEEE International Symposium on Information Theory (ISIT), Athens, Greece, 2024, pp. 2592-2597, doi: 10.1109/ISIT57864.2024.10619459.
[27] S. Wittig et al., "Demonstration of a Real-Time Testbed for D-Band Integrated Sensing and Communication," MILCOM 2024 - 2024 IEEE Military Communications Conference (MILCOM), Washington, DC, USA, 2024, pp. 641-642, doi: 10.1109/MILCOM61039.2024.10774050.
[28] G. Chai, Z. Yu, M. Nabeel, X. Wu and G. Caire, "Constant Modulus Constrained Codebook Synthesis for Self-Interference Suppression in Integrated Sensing and Communication at mmWave," 2024 Joint European Conference on Networks and Communications & 6G Summit (EuCNC/6G Summit), Antwerp, Belgium, 2024, pp. 387-391, doi: 10.1109/EuCNC/6GSummit60053.2024.10597024.
[29] Y. Zhang, J. Lin, Y. Zhao, L. Huang, Z. Gao and G. Xu, "Active RIS-Assisted Integrated Sensing and Communication Systems: Joint Receive-Transmit Beamforming and Reflection Design," 2024

IEEE 100th Vehicular Technology Conference (VTC2024-Fall), Washington, DC, USA, 2024, pp. 1-5, doi: 10.1109/VTC2024-Fall63153.2024.10758062.
[30] S. Guan, Z. Liu, R. Duan, J. Zhang and J. Bao, "Beamforming Optimization: Extended to Bidirectional Integrated Sensing and Communication System," 2024 32nd European Signal Processing Conference (EUSIPCO), Lyon, France, 2024, pp. 2177-2181, doi: 10.23919/EUSIPCO63174.2024.10715415.
[31] B. Wang, C. Jiao, Q. Zhang, K. Yu and D. Ma, "Hardware Verification and Performance Evaluation of MmWave Beam Tracking for Integrated Sensing and Communication," 2024 IEEE Wireless Communications and Networking Conference (WCNC), Dubai, United Arab Emirates, 2024, pp. 1-6, doi: 10.1109/WCNC57260.2024.10571102.
[32] Y. Jiang et al., "Coverage Analysis for Air-Ground Integrated-Sensing-and-Communication Networks," 2024 International Conference on Ubiquitous Communication (Ucom), Xi'an, China, 2024, pp. 455-459, doi: 10.1109/Ucom62433.2024.10695929.
[33] H. Taghvaee, M. Khodadadi, G. Gradoni and M. Khalily, "Fully Autonomous Reconfigurable Metasurfaces with Integrated Sensing and Communication," 2024 18th European Conference on Antennas and Propagation (EuCAP), Glasgow, United Kingdom, 2024, pp. 1-5, doi: 10.23919/EuCAP60739.2024.10501539.
[34] G. Chao, "Sensing Processing Method for Integrated Sensing and Communication in Smart Home Linkage," 2024 International Conference on Ubiquitous Communication (Ucom), Xi'an, China, 2024, pp. 516-521, doi: 10.1109/Ucom62433.2024.10695897.
[35] I. Agrawal and B. R. Manoj, "Ergodic Rate for Downlink and Uplink NOMA Aided Integrated Sensing and Communication," in IEEE Communications Letters, vol. 28, no. 12, pp. 2774-2778, Dec. 2024, doi: 10.1109/LCOMM.2024.3482852.
[36] D. Wang, Y. Zeng, Y. Wang, F. Chin, Y. Ma and S. Sun, "Pilot Design, Channel Estimation, and Target Detection for Integrated Sensing and Communication with OTFS," 2024 IEEE VTS Asia Pacific Wireless Communications Symposium (APWCS), Singapore, 2024, pp. 1-5, doi: 10.1109/APWCS61586.2024.10679290.
[37] W. Liu, X. Hou and L. Chen, "Virtual Aperture Design for Integrated Sensing and Communication (ISAC) System with Unified Antenna Structure," 2024 IEEE Wireless Communications and Networking Conference (WCNC), Dubai, United Arab Emirates, 2024, pp. 1-6, doi: 10.1109/WCNC57260.2024.10571147.
[38] X. Wang et al., "Research on Pattern Design of Integrated Sensing and Communication Reference Signal in 6G," 2024 IEEE/CIC International Conference on Communications in China (ICCC Workshops), Hangzhou, China, 2024, pp. 805-810, doi: 10.1109/ICCCWorkshops62562.2024.10693761.
[39] S. Wang, L. Chen, H. Yin and W. Wang, "Distribution on the Pareto Boundary for Integrated Sensing and Communication System," 2024 16th International Conference on Wireless Communications and Signal Processing (WCSP), Hefei, China, 2024, pp. 887-893, doi: 10.1109/WCSP62071.2024.10827104.

[40] S. Fan, H. Zhang, Y. Sun and H. Jin, "Active IRS-Enabled Integrated Sensing and Communication: Extending Sensing Coverage to Non-Line-of-Sight Areas," 2024 IEEE 100th Vehicular Technology Conference (VTC2024-Fall), Washington, DC, USA, 2024, pp. 1-5, doi: 10.1109/VTC2024-Fall63153.2024.10757627.
[41] Y. Wang, Y. Xu, J. Liao, Z. Li, J. Liu and D. Wang, "Joint SNR and Mode Coupling Estimation for Integrated Sensing and Communication in Weakly-Coupled MDM Systems," 2024 Asia Communications and Photonics Conference (ACP) and International Conference on Information Photonics and Optical Communications (IPOC), Beijing, China, 2024, pp. 1-5, doi: 10.1109/ACP/IPOC63121.2024.10809564.
[42] I. Surahmat and D. Heberling, "The Potential of Channel Impulse Response Correlation in Integrated Sensing and Communication: A Wideband Measurement Analysis," 2024 International Symposium on Antennas and Propagation (ISAP), Incheon, Korea, Republic of, 2024, pp. 1-2, doi: 10.1109/ISAP62502.2024.10846425.
[43] P. S. Bithas, G. P. Efthymoglou, A. G. Kanatas and K. Maliatsos, "UAV Selection in Aerial Integrated Sensing and Communication Networks," 2024 IEEE 100th Vehicular Technology Conference (VTC2024-Fall), Washington, DC, USA, 2024, pp. 1-5, doi: 10.1109/VTC2024-Fall63153.2024.10757892.
[44] X. Liu, T. Ratnarajah, M. Sellathurai and Y. C. Eldar, "Multimodal Learning for Integrated Sensing and Communication Networks," 2024 32nd European Signal Processing Conference (EUSIPCO), Lyon, France, 2024, pp. 1177-1181, doi: 10.23919/EUSIPCO63174.2024.10715410.
[45] J. Zhu, X. Jing and D. Zhang, "Power Optimization for Integrated Sensing and Communication in Cellular Networks," 2024 IEEE 4th International Symposium on Joint Communications & Sensing (JC&S), Leuven, Belgium, 2024, pp. 1-5, doi: 10.1109/JCS61227.2024.10646306.
[46] K. F. Haque, F. Meneghello and F. Restuccia, "Integrated Sensing and Communication for Efficient Edge Computing," 2024 20th International Conference on Wireless and Mobile Computing, Networking and Communications (WiMob), Paris, France, 2024, pp. 611-614, doi: 10.1109/WiMob61911.2024.10770523.
[47] G. -E. Kim, J. -H. Kim, D. -H. Kim, H. Kang, H. K. Son and W. -H. Lee, "Analysis of Signal Correlation in Integrated Sensing and Communication Systems: An Interference Perspective," 2024 15th International Conference on Information and Communication Technology Convergence (ICTC), Jeju Island, Korea, Republic of, 2024, pp. 1993-1996, doi: 10.1109/ICTC62082.2024.10826712.
[48] H. Ma, "Integrated Sensing and Communication - The ISAC Technology," 2024 IEEE 2nd International Conference on Sensors, Electronics and Computer Engineering (ICSECE), Jinzhou, China, 2024, pp. 225-229, doi: 10.1109/ICSECE61636.2024.10729432.
[49] J. Wang, F. Wang and D. Liu, "Adaptive Beamforming in Integrated Sensing and Communication System Based on Non-orthogonal Multiple Access," 2024 IEEE 4th International Conference on Electronic Communications, Internet of Things and Big Data (ICEIB), Taipei, Taiwan, 2024, pp. 49-52, doi: 10.1109/ICEIB61477.2024.10602624.

[50] Y. Su, Q. Cheng and Z. Liu, "Integrated Sensing and Communication for UAV Detection: A Reinforcement Learning-based Approach," 2024 IEEE Cyber Science and Technology Congress (CyberSciTech), Boracay Island, Philippines, 2024, pp. 540-543, doi: 10.1109/CyberSciTech64112.2024.00096.
[51] Y. Liu, X. Deng, N. Zhong, X. Zou, W. Pan and L. Yan, "Simulation of Constant-Envelope THz Integrated Sensing and Communication System Based on Photonics with 2D Positioning," 2024 Asia Communications and Photonics Conference (ACP) and International Conference on Information Photonics and Optical Communications (IPOC), Beijing, China, 2024, pp. 1-5, doi: 10.1109/ACP/IPOC63121.2024.10809603.
[52] J. Gong, F. Wang, Y. Wei, Q. Su and J. Xu, "Research on OFDM-based Integrated Sensing and Communication Method," 2024 IEEE 7th Information Technology, Networking, Electronic and Automation Control Conference (ITNEC), Chongqing, China, 2024, pp. 248-251, doi: 10.1109/ITNEC60942.2024.10733160.
[53] P. Tosi, M. Henninger, L. G. de Oliveira and S. Mandelli, "Feasibility of Non-Line-of-Sight Integrated Sensing and Communication at mmWave," 2024 IEEE 25th International Workshop on Signal Processing Advances in Wireless Communications (SPAWC), Lucca, Italy, 2024, pp. 331-335, doi: 10.1109/SPAWC60668.2024.10694426.
[54] C. Dou, N. Huang, Y. Wu, L. Qian and T. Q. S. Quek, "Device-to-Device Communications aided Integrated Sensing and Communication Networks: A Joint Design of Bandwidth and Power Allocations," GLOBECOM 2024 - 2024 IEEE Global Communications Conference, Cape Town, South Africa, 2024, pp. 4322-4327, doi: 10.1109/GLOBECOM52923.2024.10901771.
[55] A. Sneh, A. Tewari, S. S. Ram and S. J. Darak, "Performance Analysis of Millimeter Wave Radar Waveforms for Integrated Sensing and Communication," 2024 IEEE Microwaves, Antennas, and Propagation Conference (MAPCON), Hyderabad, India, 2024, pp. 1-5, doi: 10.1109/MAPCON61407.2024.10923140.
[56] B. Liu, J. Wu, Q. Zhang and H. Wong, "An Integrated Sensing and Communication Architecture using Reconfigurable Intelligent Surfaces for 6G Wireless Networks," 2024 15th Global Symposium on Millimeter-Waves & Terahertz (GSMM), Hong Kong, 2024, pp. 42-44, doi: 10.1109/GSMM61775.2024.10553124.
[57] H. Zhang, S. Chen, W. Meng and C. Li, "Cooperative Sensing and User-Echo Associations for Integrated Sensing and Communication Networks," GLOBECOM 2024 - 2024 IEEE Global Communications Conference, Cape Town, South Africa, 2024, pp. 1371-1376, doi: 10.1109/GLOBECOM52923.2024.10901313.
[58] C. A. Gómez-Vega, O. Y. Kolawole, M. Hunukumbure, T. Mach, M. Z. Win and A. Conti, "Device-Free Localization: Outdoor 5G Experimentation at mm-Waves," in IEEE Communications Letters, vol. 27, no. 9, pp. 2353-2357, Sept. 2023, doi: 10.1109/LCOMM.2023.3289652.
[59] Y. Dai, W. Nam, T. Luo and A. Kannan, "A Cooperative Device Free Wireless Sensing Design and Analysis for Target Position Estimation," 2022 IEEE International Conference on Communications

Workshops (ICC Workshops), Seoul, Korea, Republic of, 2022, pp. 830-835, doi: 10.1109/ICCWorkshops53468.2022.9814522.
[60] Z. Wang et al., "Visual Transformers for Cooperative Device-free Object Localization Using mmWave Signals," 2024 IEEE 100th Vehicular Technology Conference (VTC2024-Fall), Washington, DC, USA, 2024, pp. 1-6, doi: 10.1109/VTC2024-Fall63153.2024.10757641.
[61] R. Maksymiuk, M. Płotka, K. Abratkiewicz and P. Samczyński, "5G Network-Based Passive Radar for Drone Detection," 2023 24th International Radar Symposium (IRS), Berlin, Germany, 2023, pp. 1-10, doi: 10.23919/IRS57608.2023.10172437.
[62] D. Solomitckii, M. Gapeyenko, V. Semkin, S. Andreev and Y. Koucheryavy, "Technologies for Efficient Amateur Drone Detection in 5G Millimeter-Wave Cellular Infrastructure," in IEEE Communications Magazine, vol. 56, no. 1, pp. 43-50, Jan. 2018, doi: 10.1109/MCOM.2017.1700450.
[63] X. Ai, L. Zhang, Y. Zheng and F. Zhao, "Passive Detection Experiment of UAV Based on 5G New Radio Signal," 2021 Photonics & Electromagnetics Research Symposium (PIERS), Hangzhou, China, 2021, pp. 2124-2129, doi: 10.1109/PIERS53385.2021.9695141.
[64] M. I. Teo, C. K. Seow and K. Wen, "5G Radar and Wi-Fi Based Machine Learning on Drone Detection and Localization," 2021 IEEE 6th International Conference on Computer and Communication Systems (ICCCS), Chengdu, China, 2021, pp. 875-880, doi: 10.1109/ICCCS52626.2021.9449224.
[65] V. Semkin, M. Yin, Y. Hu, M. Mezzavilla and S. Rangan, "Drone Detection and Classification Based on Radar Cross Section Signatures," 2020 International Symposium on Antennas and Propagation (ISAP), Osaka, Japan, 2021, pp. 223-224, doi: 10.23919/ISAP47053.2021.9391260.
[66] C. Han, G. Zhang, B. Ji, J. Huo and H. Messer, "On the Potential of Using Emerging Microwave Links for City Rainfall Monitoring," in IEEE Communications Magazine, vol. 61, no. 11, pp. 174-180, November 2023, doi: 10.1109/MCOM.001.2200975.
[67] F. D. Diba, M. A. Samad, J. Ghimire and D. -Y. Choi, "Wireless Telecommunication Links for Rainfall Monitoring: Deep Learning Approach and Experimental Results," in IEEE Access, vol. 9, pp. 66769-66780, 2021, doi: 10.1109/ACCESS.2021.3076781.
[68] G. Verma, P. Mittal and S. Farheen, "Real Time Weather Prediction System Using IOT and Machine Learning," 2020 6th International Conference on Signal Processing and Communication (ICSC), Noida, India, 2020, pp. 322-324, doi: 10.1109/ICSC48311.2020.9182766.
[69] K. Murugan, R. K. Tiruveedhi, D. R. Ramireddygari, D. Thota and C. Neeli, "AI based Weather Monitoring System," 2022 Second International Conference on Advanced Technologies in Intelligent Control, Environment, Computing & Communication Engineering (ICATIECE), Bangalore, India, 2022, pp. 1-5, doi: 10.1109/ICATIECE56365.2022.10047380.
[70] L. Pavlopoulos, P. Michalis, M. Vlachos, A. Georgakopoulos, C. Tsiakos and A. Amditis, "Integrated Sensing Solutions for Monitoring Heritage Risks," IGARSS 2024 - 2024 IEEE International Geoscience and Remote Sensing Symposium, Athens, Greece, 2024, pp. 3352-3355, doi: 10.1109/IGARSS53475.2024.10641101.

[71] C. Han, G. Zhang, B. Ji, J. Huo and H. Messer, "On the Potential of Using Emerging Microwave Links for City Rainfall Monitoring," in IEEE Communications Magazine, vol. 61, no. 11, pp. 174-180, November 2023, doi: 10.1109/MCOM.001.2200975.
[72] M. Sadhukhan, S. Dasgupta and I. Bhattacharya, "An Intelligent Weather Prediction System Based on IOT," 2021 Devices for Integrated Circuit (DevIC), Kalyani, India, 2021, pp. 528-532, doi: 10.1109/DevIC50843.2021.9455883.
[73] S. Aliaga, A. J. Alqaraghuli and J. M. Jornet, "Joint Terahertz Communication and Atmospheric Sensing in Low Earth Orbit Satellite Networks: Physical Layer Design," 2022 IEEE 23rd International Symposium on a World of Wireless, Mobile and Multimedia Networks (WoWMoM), Belfast, United Kingdom, 2022, pp. 457-463, doi: 10.1109/WoWMoM54355.2022.00071.
[74] R. Raj et al., "Towards Efficient Confluent Edge Networks," 2024 Joint European Conference on Networks and Communications & 6G Summit (EuCNC/6G Summit), Antwerp, Belgium, 2024, pp. 1163-1168, doi: 10.1109/EuCNC/6GSummit60053.2024.10597093.
[75] T. Miyoshi et al., "“Big Data Assimilation” Toward Post-Petascale Severe Weather Prediction: An Overview and Progress," in Proceedings of the IEEE, vol. 104, no. 11, pp. 2155-2179, Nov. 2016, doi: 10.1109/JPROC.2016.2602560.
[76] S. Mandelli, M. Henninger, M. Bauhofer and T. Wild, "Survey on Integrated Sensing and Communication Performance Modeling and Use Cases Feasibility," 2023 2nd International Conference on 6G Networking (6GNet), Paris, France, 2023, pp. 1-8, doi: 10.1109/6GNet58894.2023.10317691.

II. Recent Activities in Japan

Section No.	Title / Authors
II-1	**CSI-Based Device-Free Sensing Using Deep Learning with 5G NR 28 GHz Band** Tomoki Murakami, Shinya Otsuki, NTT Corporation Yutaka Musaka, Yoshifumi Morihiro, Huiling Jiang, Satoshi Suyama, NTT DOCOMO, INC. Yasushi Maruta, NEC corporation
II-2	**Indoor Experimental Evaluation of Device-free Localization Schemes Using Channel State Information in Distributed Antenna Systems** Osamu Muta, Kyushu University Tomoki Murakami, Shinya Otsuki, NTT Corporation
II-3	**CSI2Image: CSI-to-Image Conversion using a Generative Model** Sorachi Kato, Takuya Fujihashi, Takashi Watanabe, Shunsuke Saruwatari, Osaka University Tomoki Murakami, NTT Corporation
II-4	**Use Cases for CSI Sensing with an Example of Pedestrian Movement Direction Identification** Masakatsu Ogawa, Sophia University
II-5	**Integrated Sensing and Communication (ISAC)** Chen Yan, Huawei Technologies Koshimizu Takashi, Huawei Technologies Japan
II-6	**Space-Time Synchronization** Tetsuya Ido, Nobuyasu Shiga, Motoaki Hara, Yuichiro Yano, Satoshi Yasuda, Ryuichi Ichikawa, NICT
II-7	**Experimental Evaluation of WLAN-based Device-Free Localization Using CSI in Outdoor and Large-scale Indoor Environments** Osamu Muta, Shunsuke Shimizu, Kyushu University Tomoki Murakami, Shinya Otsuki, Hanae Otani, NTT Corporation
II-8	**A Fundamental Study on the Relationship Between Pedestrian Traffic and Wi-Fi CSI with Existing Outdoor Access Points** Masakatsu Ogawa, Sophia University
II-9	**Multipath-RTI: Millimeter-Wave Radio Based Device-Free Localization** Minseok Kim, Niigata University
II-10	**Verification in an anechoic chamber toward the realization of a radio wave camera using a mobile communication system** Kazuma Tomimoto, Tomonori Ikeda, Ryo Yamaguchi, Toshiki Hozen, Syumpei Tabuchi, SoftBank Corp. Research Institute of Advanced Technology

II-1. CSI-Based Device-Free Sensing Using Deep Learning with 5G NR 28 GHz Band

Tomoki Murakami, Shinya Otsuki
NTT Corporation
Yutaka Musaka, Yoshifumi Morihiro, Huiling Jiang, Satoshi Suyama
NTT DOCOMO, INC.
Yasushi Maruta
NEC corporation

Abstract— **Integrated Sensing and Communication (ISAC) is gaining attraction as it aims to bring added value to next-generation mobile communication networks. This paper offers an overview of the device-free sensing technology, which detects target object without the need for mobile terminals, utilizing deep learning. It further introduces the effectiveness of this technology based on our experiments conducted on a radio testbed equipped with the physical layer specifications of the 5G (NR) 28 GHz band.**

II-1.1. Introduction

The Japanese Cabinet Office has advocated “Society 5.0” to realize a human-centered society that balances economic advancement with the resolution of social problems through a system that highly integrates cyberspace and physical space [1]. This system leverages artificial intelligence (AI) and machine learning (ML) to analyze vast amounts of sensor data as big data in physical space, providing feedback to humans in various forms. Sensor data plays a pivotal role in Society 5.0 and requires efficient and cost-effective integration into cyberspace. In response to this need, the Third Generation Partnership Project (3GPP) has initiated discussions on Integrated Sensing and Communication (ISAC) for the secondary use of radio waves. Defined use cases include the detection of human and animal intrusions in indoor/outdoor environments and understanding the status of automobiles and Automatic Guided Vehicles (AGVs) [2].

Sensing technologies utilizing radio waves have found widespread applications in detecting the distance and direction of objects, among other functionalities. With the current rapid advancements in AI/ML, their application scope continues to broaden, particularly in shape, motion, and gesture detections [3][4]. This paper specifically focuses on device-free sensing as a method for detecting target objects without the need for mobile terminals. It introduces a Channel State Information (CSI)-based device-free sensing method that achieves high-precision location detection of target objects through the application of a Deep Neural Network (DNN). Additionally, we demonstrate the performance of the proposed method through the results of an indoor experiment conducted on a radio testbed, equipped with the physical layer specifications of the 5G (NR) 28 GHz band [5].

II-1.2. CSI-based device-free sensing using DNN

As outlined in the reference paper [6], the integration of DNN into radio communication networks is advancing, with sensing technologies using radio waves being fundamental to this progress. This paper introduces a device-free localization method, utilizing a DNN capable of detecting the location of a target object without relying on mobile terminals [7][8]. Figure III-1.1 depicts a system model wherein the detection of objects such as humans or cars and their states is accomplished through the analysis of radio waves between Beyond 5G (B5G) base stations (BSs). The training data for this system includes the target object locations and CSI between B5G-BSs, serving as the physical information. CSI, obtained through reference signals and similar means, is vital information for demodulation processing in radio communication networks. A prediction model for the DNN, developed through supervised learning based on recurrent neural network architecture, is constructed using the locations of target objects and CSI. Subsequently, the location of the target object is determined through the prediction model and the acquired CSI. This detected location information can be stored in cyberspace as sensor data, thereby contributing to the enhancement of radio communication network quality.

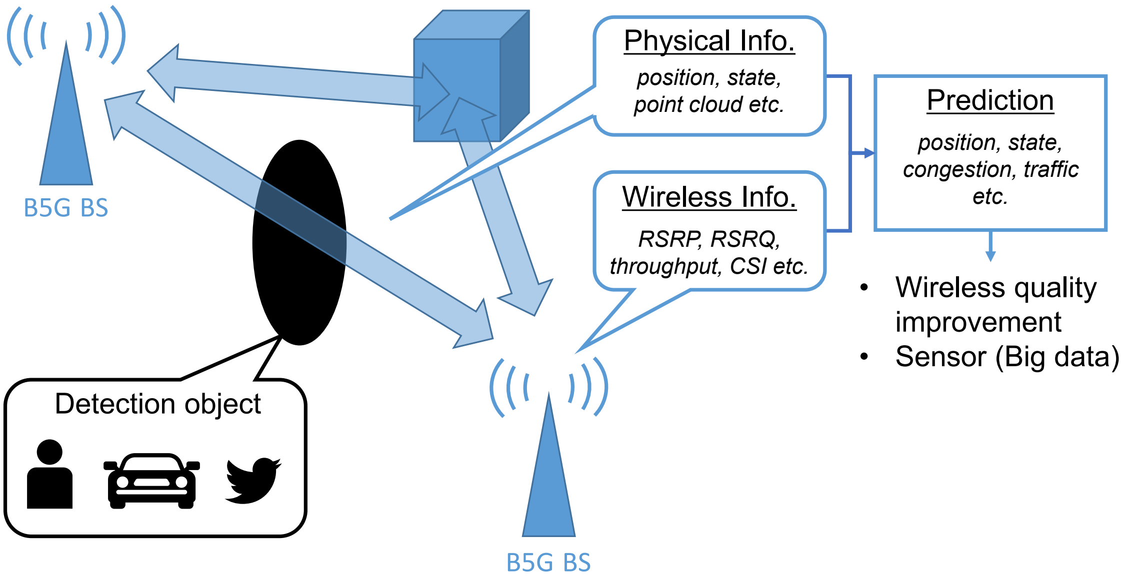

Figure III-1.1 System model.

II-1.3. Experimental results

We demonstrate the effectiveness of CSI-based device-free sensing utilizing a 28 GHz radio testbed [5]. As depicted in Figure III-1.2, the experimental setting comprises an indoor office with dimensions of 25 m × 15 m × 3.5 m and four columns. The radio testbed is configured to meet the physical specifications of 5G NR in the 28 GHz band, employing Multiple Input Multiple Output (MIMO) Orthogonal Frequency Division Multiplexing (OFDM) transmission with a 100 MHz bandwidth and a subcarrier spacing of 60 kHz. To enhance sensing accuracy, antennas for each BS are strategically distributed, as illustrated in Figure III-1.2. The CSI for 6 × 2 MIMO-OFDM is acquired at 1-millisecond intervals through reference signals exchanged between BSs. The target object in this experiment is a human body phantom adjusted to match the dielectric constant of an actual human body in the 28 GHz band. Moreover, the phantom is mounted on an AGV for automated movement within the designated area, facilitating precise location information acquisition.

Figure III-1.3 shows the cumulative distribution of the distance error between the detected location obtained from the proposed DNN-based method and the actual location. The predictive DNN model incorporates pre-acquired location information of the human body phantom and CSI from the BS. This figure highlights that the median location error for the human body phantom is approximately 0.6 m, with a root mean squared error (RMSE) of 1.1 m. While previous studies have demonstrated the effectiveness of location detection using Wi-Fi within sub-6 GHz bands, these results affirm the feasibility of location detection in the 28 GHz band.

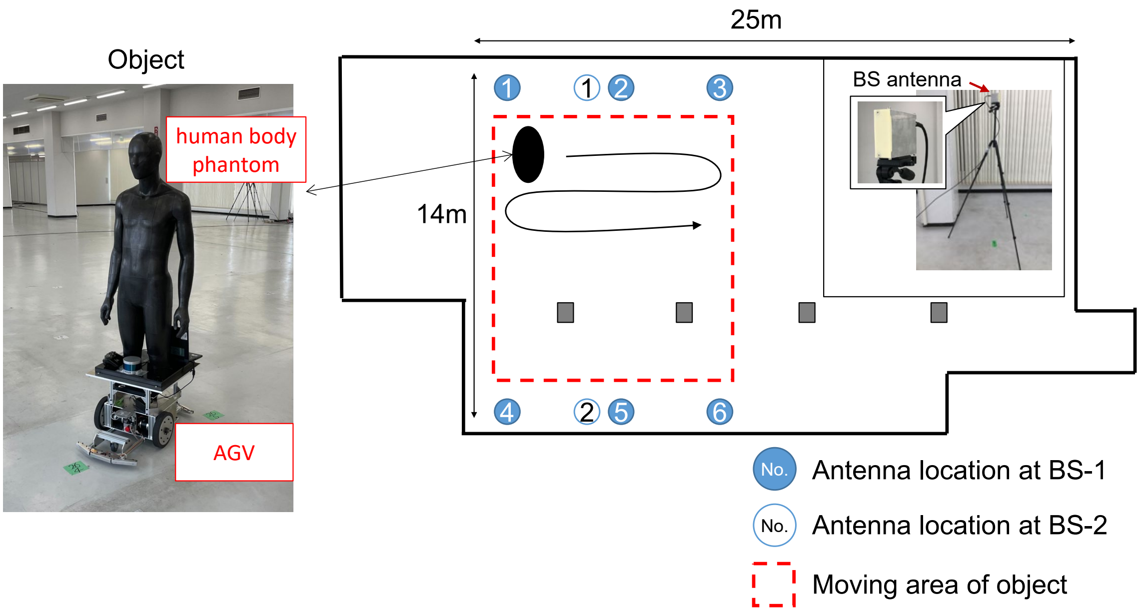

Figure III-1.2 Experimental environment.

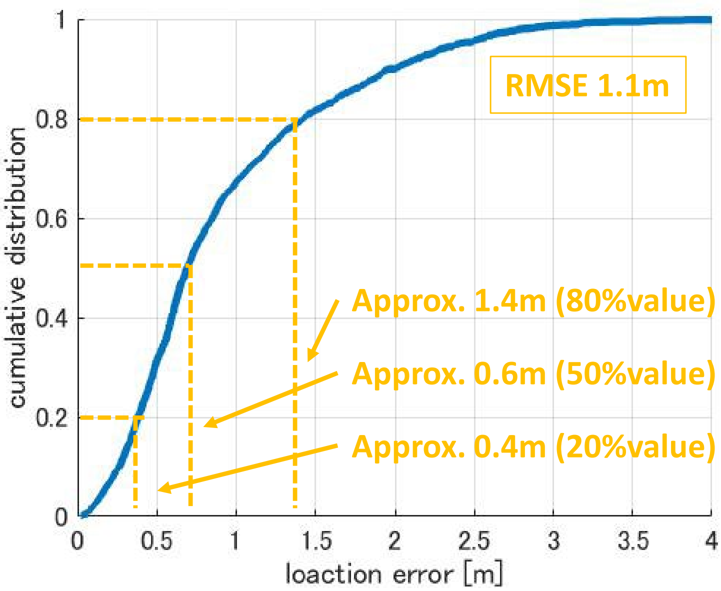

Figure III-1.3 Experimental results.

II-1.4. Conclusion

This paper outlines the CSI-based device-free sensing method for detecting a target object without the need for mobile terminals. Furthermore, we demonstrated the feasibility of achieving 1-meter-class localization through indoor experiments conducted on a radio testbed equipped with the 5G (NR) 28 GHz band. In the future, we intend to validate its application in outdoor scenarios and explore the detection capabilities for multiple objects.

REFERENCE

[1] Cabinet office, "Society 5.0", https://www8.cao.go.jp/cstp/english/society5_0/index.html

[2] 3GPP TR 22.837, "Feasibility Study on Integrated Sensing and Communication"

[3] M. Yongsen, G. Zhou, and S. Wang, "WiFi sensing with channel state information: A survey," ACM Computing Surveys, vol.52, no.46, June 2019.

[4] J. Liu, H. Liu, Y. Chen, Y. Wang, and C. Wang, "Wireless sensing for human activity: A survey," IEEE Communications Surveys & Tutorials, vol.22, no.3, Aug. 2019.

[5] NTT, NTT DOCOMO, NEC, "World's first successful demonstration of distributed MIMO that continues wireless connections in the 28 GHz band by eliminating shielding issues," https://group.ntt/en/newsrelease/2022/10/31/221031a.html

[6] C. Zhang, P. Patras, and H. Haddadi, "Deep learning in mobile and wireless networking: survey," IEEE Communications surveys & tutorials, vol.21, no.3, March 2019.

[7] R. Kudo, K. Takahashi, N. Nagata, T. Murakami, T. Ogawa, and K. Takasugi, "Wireless Link Quality Prediction Using Physical Space Information based on Deep Learning," IEICE transaction, J105-B, no. 10, Oct. 2022 (Japanese).

[8] R. Kudo, K. Takahashi, T. Murakami, H. Yoshioka, and T. Ogawa, "RNN Position Estimation using a Single WLAN AP and Performance Evaluation," Proc. the 2021 IEICE Society Conference, B-15-41, 2021 (Japanese).

II-2. Indoor Experimental Evaluation of Device-free Localization Schemes Using Channel State Information in Distributed Antenna Systems

Osamu Muta, Kyushu University

Tomoki Murakami, Shinya Otsuki, NTT Corporation

Abstract—**Wireless communication system-based localization techniques that use channel state information (CSI) have attracted much attention. Performance of the CSI-based localization schemes depends strongly on the selected feature information and antenna placement. Herein, we present a real-time CSI-based device-free localization scheme for distributed antenna systems, where CSI feedback frames are collected and used as a dataset for machine learning (ML)-based localization. Experimental results confirmed that the developed localization scheme is effective for detecting a target in an indoor environment. We also discuss how much performance improvement can be expected when antenna placement is given properly.**

II-2.1. Introduction

Wireless sensing is a key technology supporting the evolution of wireless communication for Beyond-5G and 6G networks [1]. The basic principle of wireless sensing is to characterize the status and behavior of a target object as radio propagation characteristics in wireless channels; a received signal strength indicator (RSSI) and channel state information (CSI) are useful as feature information for wireless sensing. Recently, indoor device-free object detection approaches using radio signals of existing wireless communication infrastructure, have been investigated [2]-[7], where large amounts of CSI in the frequency and spatial domains are acquired simultaneously using multi-input multi-output (MIMO) transmission with orthogonal frequency division multiplexing (OFDM). In [5]-[7], IEEE802.11ac-based wireless local area network (WLAN)-based device-free indoor object detection schemes were proposed, by which CSI feedback frames in WLANs were collected and analyzed to detect a target object and its behavior. However, the performance achieved by the CSI-based approaches depends strongly on the antenna placement and the surrounding propagation environment.

This paper introduces our recent studies of wireless communication system-based indoor device-free localization where feedback beamforming weights are used as effective feature data for machine learning (ML)-based object detection and localization. Experiment results demonstrate that our developed algorithm works well with small datasets in an indoor environment when distributed antenna placement is accomplished properly.

II-2.2. CSI-based localization approaches

Figure III-2.1 presents an illustration of the principles of device-free localization in wireless communication systems where the CSI between the base station (BS) and the terminal is affected by the target presence. Consequently, it is expected to detect the target by learning the relation between the states of the target and of the wireless channel without requiring that the target have wireless devices. However, a challenging hurdle is acquisition of a sufficient amount of CSI from environments. An effective method is to use CSI in existing WLAN systems [5].

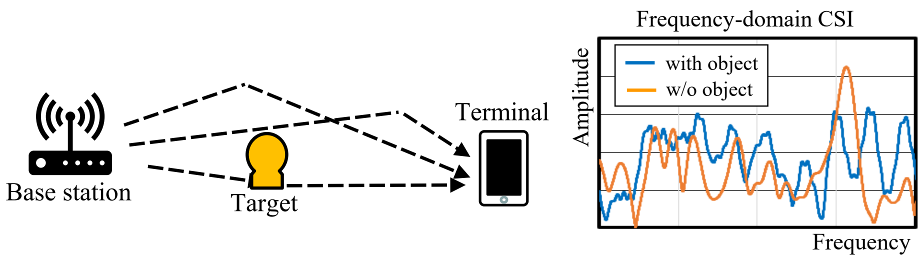

Figure III-2.1 Principles of device-free localization using CSI.

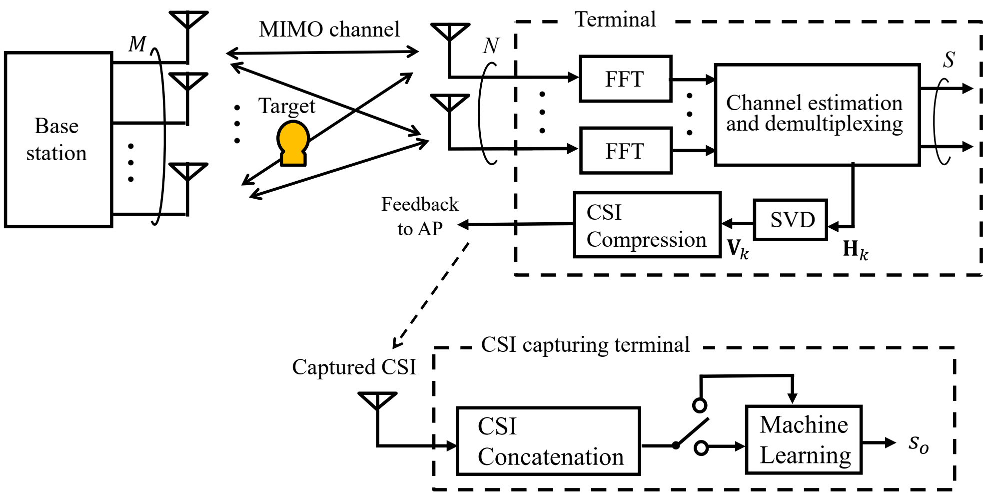

Figure III-2.2 Block diagram of the device-free object detection system.

Figure III-2.2 portrays a block diagram of the object detection and localization system consisting of an BS, a terminal, and a CSI-capturing terminal, where M, N, and S respectively denote the numbers of transmit antennas, received antennas, and streams. On the terminal side, after channel estimation, a compressed version of a right-singular matrix obtained by singular value decomposition of the channel matrix is fed back to the BS side as beam-forming weights (BFWs). After the CSI-capturing terminal collects feedback frames sent by the terminal, it extracts the compressed CSI samples and uses them for ML-based localization [5]-[7]. To improve the localization performance, we developed an effective lightweight algorithm with a small dataset [6], where current and past BFWs are concatenated as single data to build more accurate feature data. In addition, a frequency-domain sampling-based CSI compression [6] is adopted to minimize the dataset and the required complexity. After applying frequency-domain sampling and concatenating multiple BFWs as single feature data, they are used for both off-line training and for on-line detection.

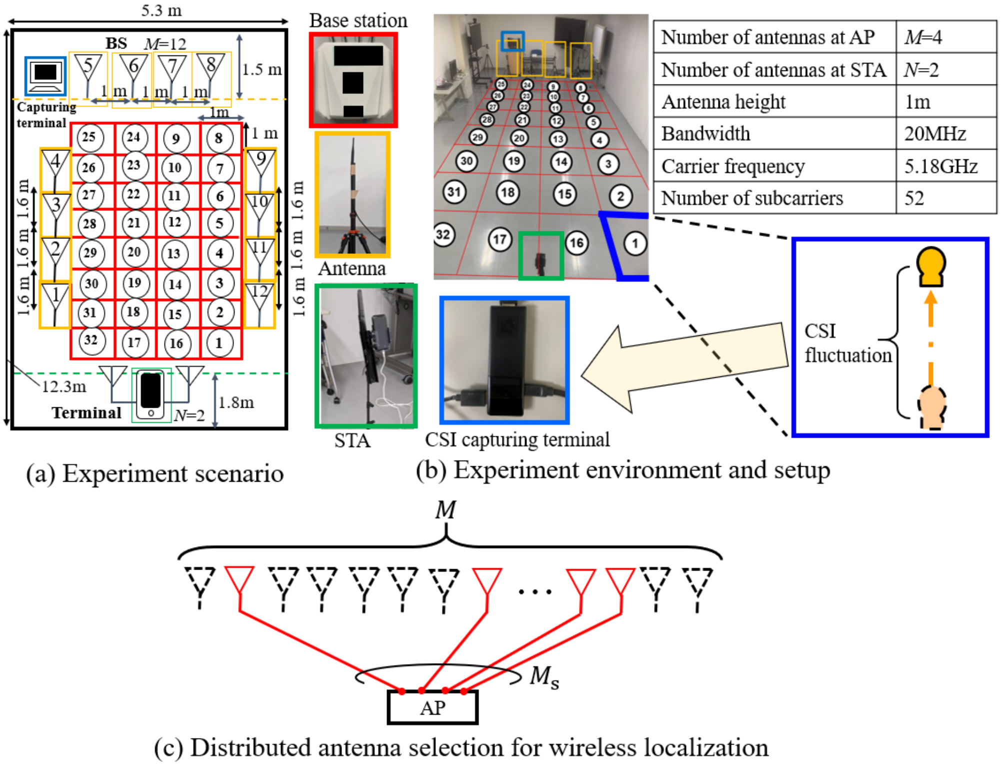

Figure III-2.3 Experiment scenario and setup.

II-2.3. Experiment scenario and results

To clarify the effectiveness of the developed algorithm in a real environment, we conducted experimental evaluations of indoor localization with the developed algorithm. The experiment scenario and setup using IEEE802.11ac-based WLAN [8] are depicted in Figure III-2.3. Details of the experiments are presented in an earlier report of the relevant literature [7]. The detection area is divided into R regions labeled as 1, …, R=32. For this experiment, we consider a multi-class classification problem to detect the location (label) of a single target object. Random Forest model is used and built by off-line training with measured CSI. We evaluate the detection probability, which is defined as a conditional probability that the ML result is the same as the actual label number where a target person is located in one of the R=32 labeled areas. In this scenario, the detection probability is evaluated when a few (M_s=4) antennas are selected among numerous distributed antennas (M=12) to elucidate the relation between antenna placement and the detection probability.

Figure III-2.4(a) presents the detection probabilities for all possible antenna patterns where M_s=4 antennas are selected among M=12. The total number of antenna combinations is 495. The horizontal axis index shows the antenna pattern numbers sorted from left to right in descending order of the average detection probability. The result indicates that about 20-point performance improvement can be confirmed for the antenna patterns with the maximum (best) and minimum (worst) detection probabilities. Heatmaps of the best 5 and the worst 5 area-wise detection probabilities are also shown respectively in Figure III-2.4(b) and Figure III-2.4(c). Results imply that a lower detection probability (better performance) tends to be obtained when the AP antenna positions are distributed.

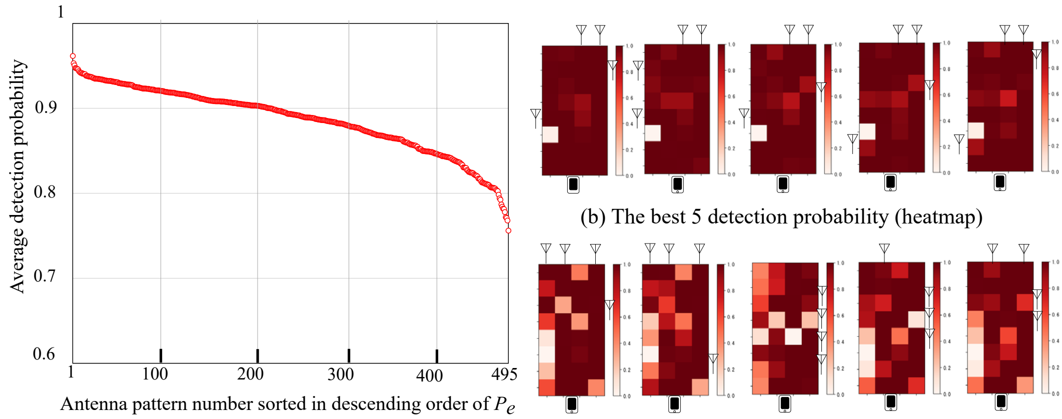

(a) Average detection probability for different antenna positions

(b) The best 5 detection probability (heatmap)

(c) The worst 5 detection probability (heatmap)

Figure III-2.4 Average detection probability for selected antenna positions.

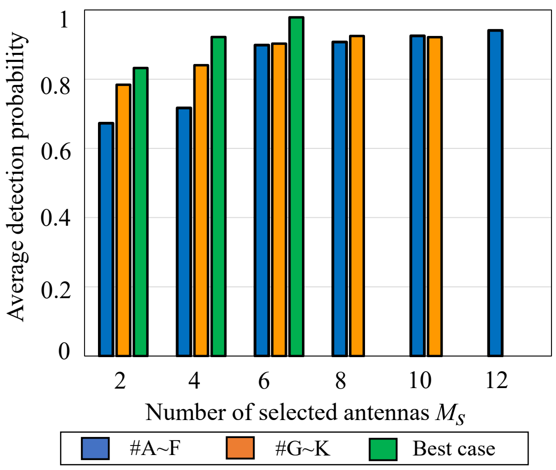

	Selected antenna numbers in Fig.3
A	(5, 6)
B	(5, 6, 7, 8)
C	(1, 2, 5, 6, 7, 8)
D	(1, 2, 3, 4, 5, 6, 7, 8)
E	(1, 2, 3, 4, 5, 6, 7, 8, 11, 12)
F	(1, 2, 3, 4, 5, 6, 7, 8, 9, 10, 11, 12)
G	(3, 5)
H	(3, 5, 6, 12)
I	(1, 3, 5, 7, 10, 12)
J	(1, 3, 4, 5, 6, 7, 10, 12)
K	(1, 3, 4, 5, 6, 7, 8, 10, 11, 12)

Figure III-2.5 Average detection probability in case of Ms = 2, 4, 6, 8, 10, and 12.

Figure III-2.5 portrays the detection probability for a particular antenna placement in terms of the number of selected antennas. The table in the figure presents the selected antenna elements for each case, which corresponds to the antenna numbers in Figure III-2.4(a). This figure shows that distributing the antenna placement improves the localization performance, which consequently maximizes the average detection probability. Results indicate that the overall detection probability improves as M_s increases because M_s becomes greater, and because more features are used for ML-based localization. This finding implies that, if using the optimal antenna pattern for M_s=4 is possible, then average detection probability comparable to the case of M_s=12 can be achieved.

II-2.4. Conclusion

As described herein, we introduced a device-free localization scheme using concatenated CSI in wireless communication systems with distributed antennas. Experiment results demonstrate that the developed scheme works well with small datasets in an indoor environment scenario. Moreover, we have demonstrated that the antenna placement strongly affects the achievable localization performance in an indoor environment. Developing object detection algorithms with a more powerful ML model is left as a subject for our future work.

Acknowledgments

We thank Mr. Junsuke Izumi and Mr. Shunsuke Shimizu, master course students at Kyushu University, for their contributions to this research.

REFERENCE

[1] "White Paper 5G Evolution and 6G (Version 5)," NTT DOCOMO, Inc., Jan. 2023, https://www.docomo.ne.jp/english/binary/pdf/corporate/technology/whitepaper_6g/DOCOMO_6G_White_PaperEN_v5.0.pdf

[2] A. Khalajmehrabadi, N. Gatsis, and D. Akopian, "Modern WLAN Fingerprinting Indoor Positioning Methods and Deployment Challenges," IEEE Communications Surveys & Tutorials, vol. 19, no. 3, pp. 1974–2002, Oct. 2017.

[3] H. Jiang, C. Cai, X. Ma, Y. Yang, and J. Liu, "Smart Home Based on WiFi Sensing: A Survey," IEEE Access, vol. 6, pp. 13317–13325, March 2018.

[4] H. Zhu, F. Xiao, L. Sun, R. Wang, and P. Yang, "R-TTWD: Robust Device-free Through-the-wall Detection of Moving Human with WiFi," IEEE Journal on Selected Areas in Communications, vol. 35, no. 5, pp. 1090-1103, March 2017.

[5] T. Murakami, M. Miyazaki, M. Ishida, and A. Fukuda, "Wireless LAN Based CSI Monitoring System for Object Detection," MDPI Electronics, Nov. 2018.

[6] O. Muta, K. Takata, K. Noguchi, T. Murakami, and S. Otsuki, "Device-Free WLAN Based Indoor Localization Scheme with Spatially Concatenated CSI and Distributed Antennas," IEEE Trans. Vehicular Technology, vol. 72, no. 1, pp. 852-865, Jan. 2023.

[7] S. Shimizu, O. Muta, K. Noguchi, T. Murakami, and S. Otsuki, "Performance of WLAN-based Object Detection with Distributed Antenna and Spatially Concatenated CSI," Proc. IEEE VTC-Fall 2023 Workshop, Oct. 2023.

[8] IEEE Computer Society, IEEE 802.11-2016, LAN/MAN Standards Committee, 2016.

II-3. CSI2Image: CSI-to-Image Conversion using a Generative Model

Sorachi Kato, Takuya Fujihashi, Takashi Watanabe, Shunsuke Saruwatari
Osaka University
Tomoki Murakami
NTT Corporation

Abstract—**Wireless sensing studies based on channel state information (CSI) continue to be successful in various sensing tasks. However, we still have no clear answer to what extent we can extract the environmental parameters of physical space from CSI. We proposed CSI2Image to address such a challenging issue. It converts CSI observations into RGB images corresponding to the physical space using generative adversarial network (GAN) architecture. The generated RGB images intuitively show the relationship between the CSI observations and the physical space, and potentially help us to extract many environmental parameters for multi-purpose sensing system.**

II-3.1. Introduction

Wireless sensing is becoming an increasingly attractive sensing technique in Beyond 5G and 6G networks due to its potential to solve issues associated with conventional sensor-based sensing and its ability to provide extensive, precise, and non-invasive sensing. CSI based sensing is crucial for integrating communication and radar sensing. Many studies have shown its adaptability for various sensing tasks, including activity recognition [1], [2], vital signal sensing [3], [4], and localization [5], [6]. However, CSI based sensing faces an open issue: how information in physical space is reflected in CSI observations. To address this, further research is needed to better understand the relationship between physical space and CSI observations.

To tackle the challenging issue, this paper introduces CSI2Image [7]. It converts CSI observations in a more intuitive format, RGB images, allowing us to comprehensively understand how CSI reflects the physical space. CSI2Image generates images of the physical space from CSI observations using GAN architecture in an end-to-end manner. Experiments demonstrated that the well-trained CSI2Image can generate the snapshots of the physical space from the CSI observations by extracting rich information from them. In addition, thanks to the advancement of sophisticated image recognition techniques, we can extract the various properties of the physical space using the generated images and image recognition techniques.

II-3.2. CSI2Image

Figure III-3.1 shows the overview of the proposed CSI2Image. The basic architecture is based on DCGAN [8], thus the models are trained in an adversarial manner: the generator aims to generate realistic images, while the discriminator tries to distinguish between real and generated images. The generator takes both CSI observations and latent variables from a standard normal distribution as input.

In addition, it is assumed that we have a pair of time-synchronized CSI observations and images of the targeted physical space.

We experimentally confirmed that simply introducing DCGAN does not lead to satisfactory results. We proposed a unique training loop called "Hybrid Learning", which aims to ensure the generalizability of the networks for both image generation and real/fake determination, as well as obtaining the precise mapping from CSIs to the images. Figure III-3.2 shows the three different training steps included in the Hybrid Learning. The first step is CSI2Image Learning, where the generator is supervised trained using CSI observation and their corresponding images, followed by Discriminator Learning, where the discriminator is trained with real images and generated images, but this time the generator generates images from random latent variables. Finally, after every *K* iteration, Generality Learning is triggered to update the parameters of networks and deceive the discriminator with the images generated by CSI observations. The generator acquires the mapping from the probability field of CSI to that of the image domain while avoiding overfitting to the training dataset through the combination of direct supervision and adversarial training. The training loop successfully displays the surrounding environment in the physical space containing in CSI observations in RGB images. To extract the properties of the physical space from the images, we can employ existing vision-based object detection techniques like YOLO [9] according to the task specification.

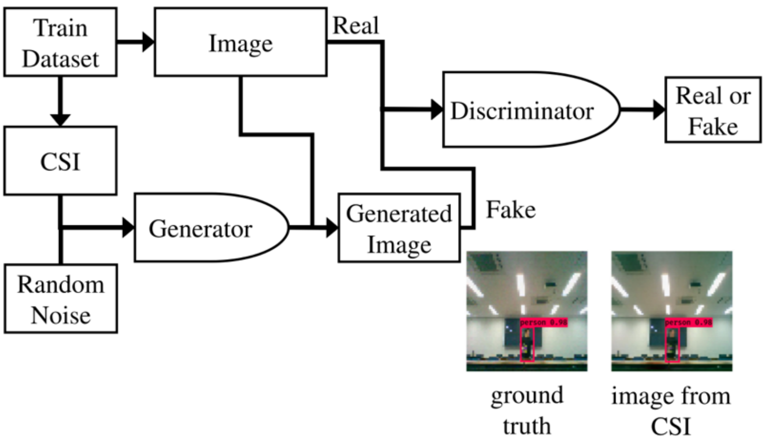

Figure III-3.1 The overview of CSI2Image.

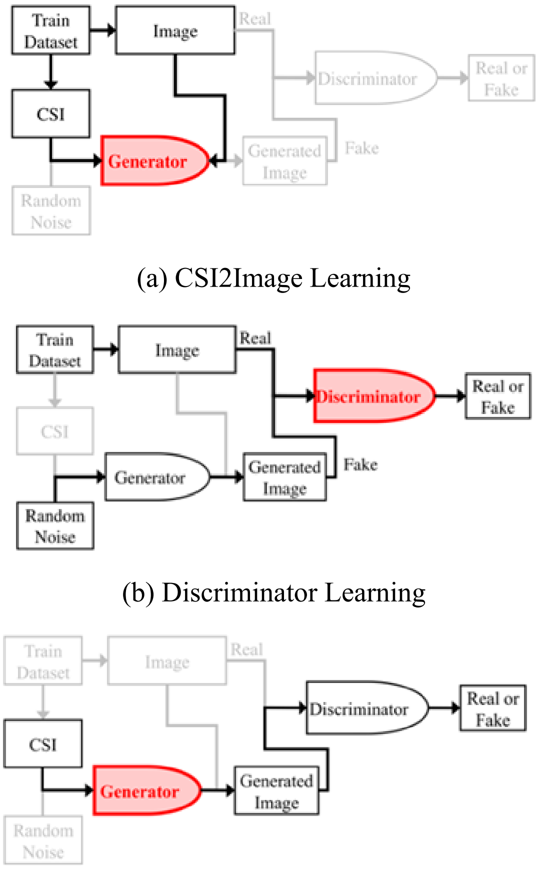

(c) Generality Learning

Figure III-3.2 The proposed hybrid learning.

II-3.3. Evaluation

To demonstrate the performance of CSI2Image to accurately generate RGB images of an indoor space from CSI observations and its performance in different sensing tasks, we conducted two experiments: object classification and human location classification. As shown in Figure III-3.3, CSI2Image successfully generated the RGB images and achieved over 90% accuracy for both tasks. Especially for human location classification task, we compared the efficiency of our proposed Hybrid Learning compared to supervised learning only with the generator (gonly) and original DCGAN training scheme (gan). Experimental results show that Hybrid Learning outperforms the other two methods in terms of detection rate, similarity score between generated images and ground truth, bounding box confidence scores, and classification accuracy. This advantage is even more pronounced in more complex scenarios involving two people.

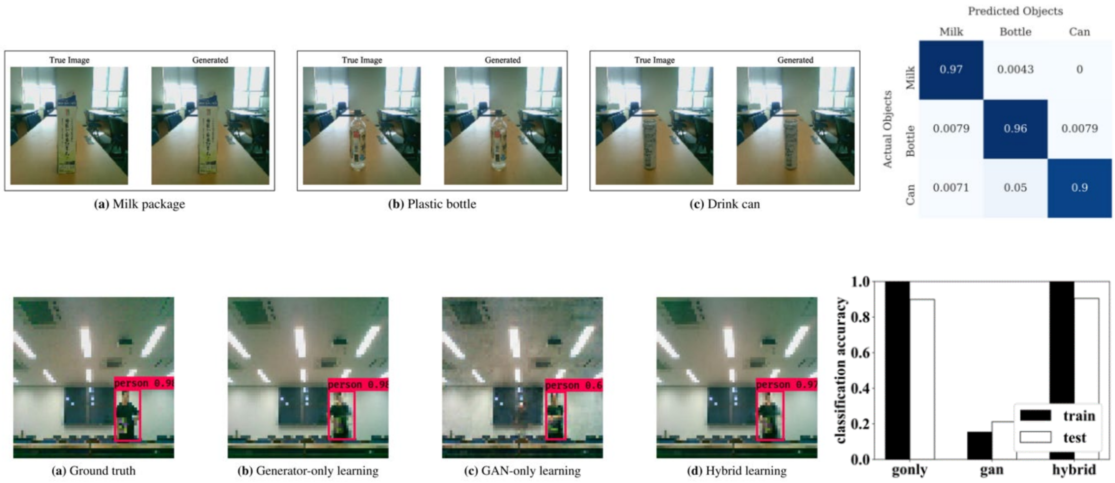

Figure III-3.3 Qualitative and quantitative evaluation for different sensing tasks.
(top) Object classification, (bottom) Human location classification.

II-3.4. Conclusion

This paper introduced the overview of CSI2Image, a GAN-based CSI-to-image conversion method. We demonstrated that the combination of direct supervision and adversarial training successfully achieves the conversion. The conversion not only helps us to represent physical information CSI has in a more explicable format but also helps us to construct multi-purpose sensing system with the vision-based detection techniques.

Acknowledgements

This work was supported in part by the Japan Society for the Promotion of Science (JSPS) KAKENHI under Grant JP19H01101 and Grant JP17KT0042, and in part by the JST PRESTO, Japan, under Grant JPMJPR2032.

REFERENCE

[1] M. Muaaz *et al.*, “Wi-Sense: a passive human activity recognition system using Wi-Fi and convolutional neural network and its integration in health information systems,” *Ann. Telecommun.*, vol. 77, no. 3, pp. 163–175, Apr. 2022.

[2] W. Meng *et al.*, “GrapHAR: A Lightweight Human Activity Recognition Model by Exploring the Sub-carrier Correlations,” *IEEE Trans. Wireless Commun.*, pp. 1–1, 2023.

[3] Z. Guo *et al.*, “BreatheBand: A Fine-grained and Robust Respiration Monitor System Using WiFi Signals,” *ACM Trans. Sen. Netw.*, vol. 19, no. 4, pp. 1–18, May 2023.

[4] Y. Li *et al.*, “DiverSense: Maximizing Wi-Fi Sensing Range Leveraging Signal Diversity,” *Proc. ACM Interact. Mob. Wearable Ubiquitous Technol.*, vol. 6, no. 2, pp. 1–28, Jul. 2022.

[5] X. Zhang *et al.*, "AutoLoc: Toward Ubiquitous AoA-Based Indoor Localization Using Commodity WiFi," *IEEE Trans. Veh. Technol.*, vol. 72, no. 6, pp. 8049–8060, Jun. 2023.

[6] Z. Wang *et al.*, "Single-target real-time passive WiFi tracking," *IEEE Trans. Mob. Comput.*, vol. 22, no. 6, pp. 3724–3742, Jun. 2023.

[7] S. Kato *et al.*, "CSI2Image: Image Reconstruction From Channel State Information Using Generative Adversarial Networks," *IEEE Access*, vol. 9, pp. 47154–47168, 2021.

[8] A. Radford *et al.*, "Unsupervised Representation Learning with Deep Convolutional Generative Adversarial Networks," *arXiv [cs.LG]*, Nov. 19, 2015.

[9] J. Redmon *et al.*, "You only look once: Unified, real-time object detection," *CVPR*, 2016, pp. 779–788.

II-4. Use Cases for CSI Sensing with an Example of Pedestrian Movement Direction Identification

Masakatsu Ogawa
Sophia University

Abstract—**The original purpose of communication is to convey information. Channel state information (CSI) is used for high-speed transmission and can also function as a sensor. Adding sensing ability to the communication function is expected to open up new services and applications. This paper describes use cases for CSI sensing from the perspectives of commercial products and my research, specifically pedestrian movement direction identification.**

II-4.1. Introduction

Wireless communication has traditionally been used to carry information through space as a medium. Most wireless communication systems currently use MIMO-OFDM transmission to achieve high-speed transmission rates. This method uses channel state information (CSI) that indicates the radio propagation condition between the transmitter and receiver. CSI can also be used as a sensor since it indicates the spatial information between a transmitter and receiver. The sensing using this information corresponds to incorporating sensing into communication, which has been discussed in "Beyond 5G and 6G" and "IEEE802.11 wireless LAN". The technical terms for this are integrated sensing and communication (ISAC) and joint sensing and communication (JSAC). However, most current wireless communication chipsets do not provide an interface for users to obtain CSI.

While research activity for CSI sensing is currently high, the number of commercial products for Wi-Fi sensing is rare. In my opinion, the reason is that the service requirements of use cases are strict, and the requirements are not entirely satisfied due to the uncertainty of radio propagation. Compared with RSSI, which also indicates the radio propagation condition, CSI has a higher reproducibility; thus, the use of CSI is suitable for sensing. The disadvantage of CSI is that it depends on the transmitter's and receiver's location. When the location changes, the CSI also differs from the change before its location.

IEEE802.11bf discusses use cases for sensing [1] but does not confirm the feasibility. The paper describes use cases of CSI sensing applications from commercial products and my research, including advantages and disadvantages from the feasibility viewpoint.

II-4.2. Use cases in IEEE802.11bf and commercial products

The difference between mobile communication and wireless LAN is the coverage area. The use cases differ depending on whether the sensing target exists in an outdoor public space or an indoor room. CSI indicates the radio propagation condition between the transmitter and receiver. Therefore, detecting a specific sensing target is difficult in an outdoor public space because of the wide area.

IEEE802.11bf discusses use cases for existing wireless LAN standards, which operate at 2.4GHz, 5GHz, 6GHz, and 60GHz [1]. The range resolution relates to the signal bandwidth, i.e., the frequency band. The specific use case for the high-frequency band, i.e., 60GHz, is high-resolution sensing, e.g., gesture recognition (hand or figure movement), and for the low-frequency band, is low-resolution sensing, e.g., human presence and motion detection [2]. Among them, CSI sensing mainly corresponds to low-resolution sensing. The use cases discussed in IEEE802.11bf are as follows: Room sensing, Gesture recognition for full-body movement, Health care, and Car sensing.

I found some information about the feasibility of the above use cases. Hex Home by Origin Wireless is a commercial product for room sensing and healthcare [3]. Specifically, room sensing is used for home security by detecting intruders and is also for home monitoring of older people and/or children. The CSI variation is used to detect human movement. Healthcare is used for measuring breathing rate using the CSI periodicity. Wiz product named SpaceSense by Signify is another commercial product that corresponds to room sensing, i.e., a smart light [4]. This light control uses the CSI variation relating to the detection of human movement. Although I could not confirm whether car sensing by Murata Manufacturing has been commercialized, CSI sensing is used to detect the presence of a child in the car by measuring movement detection and breathing rate [5]. Note that the accuracy of breathing rate measurement depends on the location of the transmitter and receiver.

Figure III-4.1 shows the relationship between use cases and the purpose of the product. CSI variation is used for presence detection, and there are many examples of its application. Combining presence detection and breathing rate measurement for intruder detection is possible, but I could not find such a product.

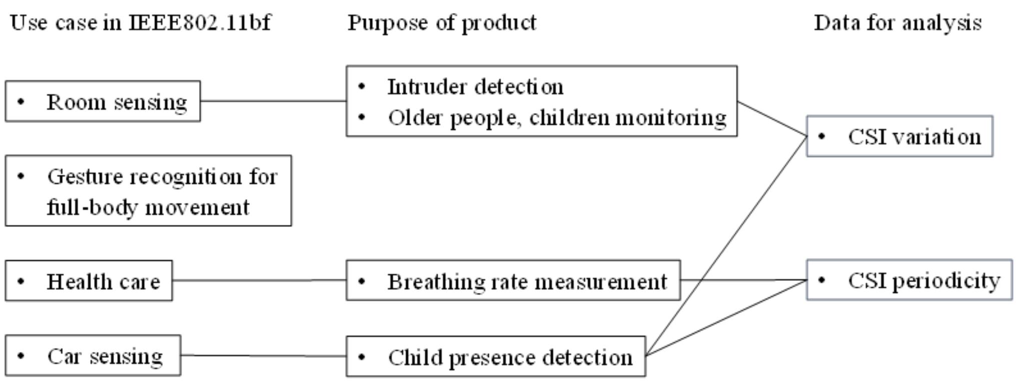

Figure III-4.1 Relationship between use cases and the purpose of products.

II-4.3. Use cases in my research

My research aims to investigate the potential of CSI sensing without considering the user's needs. Basically, the commercial products mentioned above do not require machine learning. Based on my experience with Wi-Fi, use cases for CSI sensing can be categorized into those that require machine learning and those that do not.

CSI sensing can be used for various applications without machine learning. Here are some examples of CSI sensing use cases that do not require machine learning: breathing rate measurement [6], people counting using breathing rate measurement [6], and propeller rotation speed measurement [7].

CSI sensing can also be used with machine learning for more advanced applications such as human activity recognition [8], material identification [9], pedestrian movement direction identification [10], human location estimation [11], water height estimation in a bottle [12], pose estimation [13], and laundry dryness estimation [14].

II-4.4. Pedestrian movement direction identification

Pedestrian movement direction identification is one of the use cases for CSI sensing. Nowadays, access points are often installed on the ceilings of offices and are connected to Ethernet or wireless mesh networks. In the future, if it becomes possible to measure CSI from communication between access points, it will be possible to estimate human flow.

Suppose consider a crossroads in a hallway. As shown in Figure III-4.2, one transmitter and three receivers are installed. Due to cost constraints, it is necessary to reduce the number of receivers as much as possible. There are 13 types of movement directions: four entrances to the crossroads and three exits from the crossroads per entrance. In addition to the twelve conditions, there is the condition that no humans are at the crossroads. Three people walked ten times for CSI measurements for each direction, resulting in 30 samples per direction. Including the case where no humans are at the crossroads, the total number of samples is 390. If the CSI differs in every direction, it is necessary to pay attention to the time series of CSI. Therefore, LSTM is used as a machine learning algorithm to classify the 13 types of movement directions, and accuracy is evaluated by leave-one-out cross-validation.

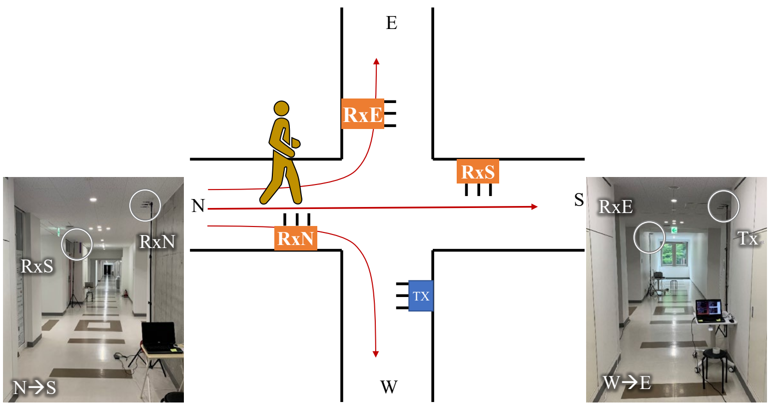

Figure III-4.2 Experimental environment.

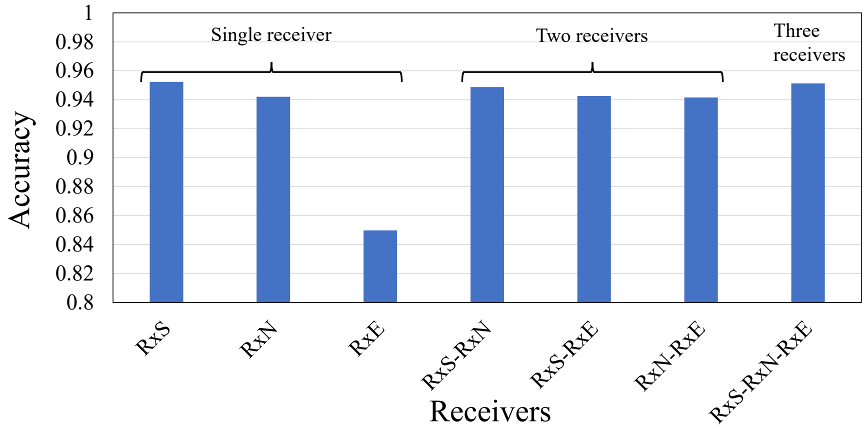

Figure III-4.3 Experimental result.

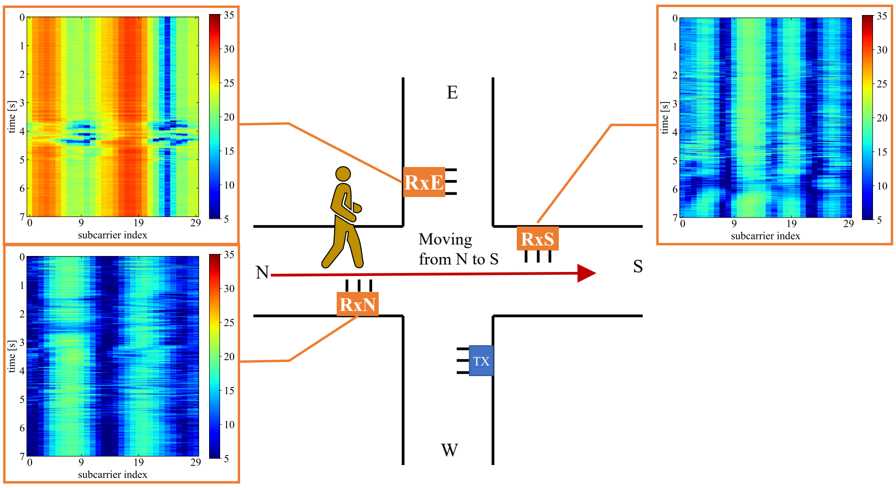

Figure III-4.4 CSI at each receiver.

The accuracy of the difference in the number of receivers is shown in Figure III-4.3. The accuracy improves with the number of receivers and is over 90% when the number of receivers is two or three. When the receiver is only RxE, the accuracy is less than 90%. Figure III-4.4 shows the time-series CSI in three receives. When a human walks from N to S, the CSI fluctuation at only RxE is short. Because of the short time of the CSI fluctuation, it isn't easy to distinguish when a human walks from N to S and when a human walks from S to N. The confusion matrix using only RxE is shown in Figure III-4.5, where the label indicates direction and "nothing" indicates no human exists. I found that the estimation error occurs between StoN and NtoS. Therefore, the receiver at a non-line-of-sight location from the transmitter needs to be set to achieve higher accuracy.

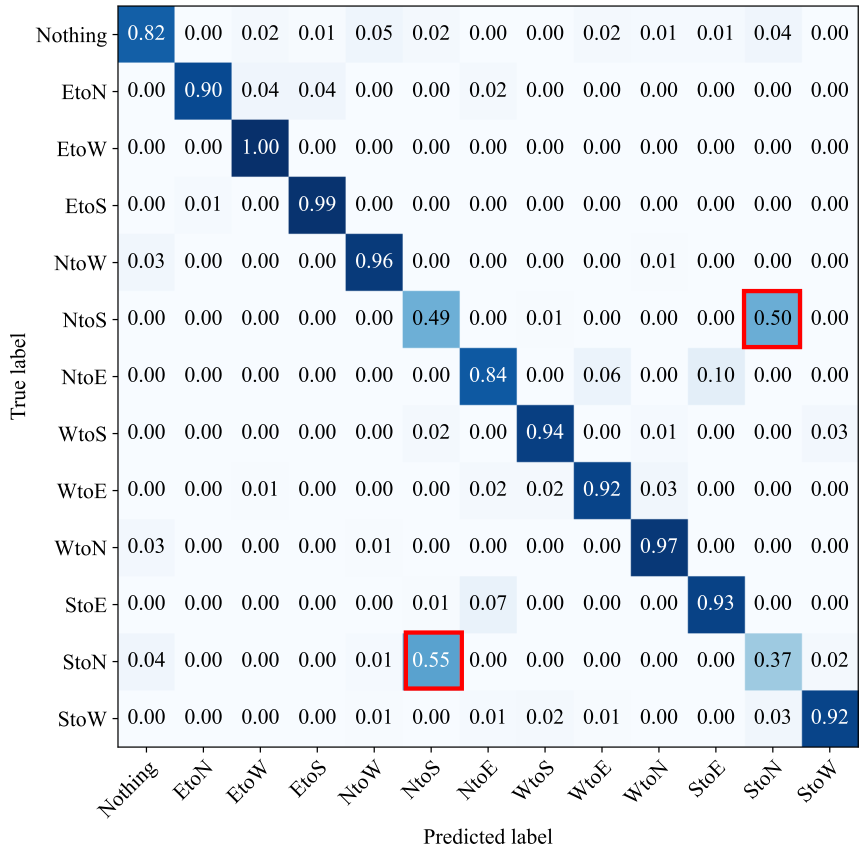

Figure III-4.5 Confusion matrix at RxE.

II-4.5. Conclusion

The paper describes use cases for CSI sensing from commercial products and my research, specifically pedestrian movement direction identification. Although only some commercial products utilize CSI sensing, various services are expected to be created in the future by utilizing this technology.

REFERENCE

[1] Assaf Kasher, et al, "WiFi Sensing Uses Cases," doc.: IEEE 802.11-20/1712r2, January 2021.
[2] Claudio da Silva, et al., "Wi-Fi sensing: Usages, requirements, technical feasibility and standards gaps," doc.: IEEE 802.11-19/1293r0, July 2019.
[3] Origin Wireless, Hex home. https://myhexhome.com/
[4] Signify, Wiz. https://www.wizconnected.com/en-us/explore-wiz/spacesense
[5] Murata Manufacturing, Wi-Fi sensing for child presence detection. https://solution.murata.com/en-global/technology/child-presence-detection
[6] R. Tokumine, M. Ogawa, "Human Counting by Estimating Breathing Rate using Wi-Fi CSI," Proc. IEICE Tech. Rep., vol. 122, no. 341, SeMI2022-78, pp. 30-33, Jan. 2023 (Japanese).

[7] M. Ogawa, T. Takahashi, "Propeller's Rotational Speed Measurement by WLAN sensing," IEEJ Trans. on Industry Applications, vol. 142, no. 12, pp. 941-947, Dec. 2022 (Japanese).
[8] M. Ogawa, H. Munetomo, "Wi-Fi CSI-Based Outdoor Human Flow Prediction Using a Support Vector Machine," Sensors, vol. 20, no. 7, 2141, 2020.
[9] Y. Tian, M. Ogawa, "Material Identification of Moving Objects by Wi-Fi Sensing Using Machine Learning," Proc. of ICETC 2021, Dec. 2021.
[10] K. Isono, M. Ogawa, "CSI-based Crossroads Movement Direction Identification using Ceiling-mounted APs," Proc. the 2022 IEICE General Conference, B-15-28. 2022 (Japanese).
[11] S. Usaka, M. Ogawa, "Comparison of Position Estimation Accuracy in Polar and Rectangular Coordinate Systems Using Wi-Fi CSI," Proc. of APWCS 2023, Aug. 2023.
[12] S. Nishino, M. Ogawa, "Water Height Estimation by Wi-Fi CSI independent of Bottle Size," Proc. IEICE Tech. Rep., vol. 122, no. 341, SeMI2022-85, pp. 57-60, Jan. 2023 (Japanese).
[13] Y. Yamahata, M. Ogawa, "Human Pose Estimation by Wi-fi CSI using RGB-D Camera," Proc. the 2022 IEICE General Conference, B-15-26. 2022 (Japanese).
[14] M. Ogawa, "A Study on Dry Estimation of Laundry by Wi-Fi Sensing," Proc. the 2023 IEICE Society Conference, B-15-5, 2023 (Japanese).

II-5. Integrated Sensing and Communication (ISAC)

Chen Yan,
Huawei Technologies
Koshimizu Takashi
Huawei Technologies Japan

***Abstract*—6G will serve as a distributed neural network for the future Intelligence of Everything. Network Sensing and Native AI will become two new usage scenarios in the era of connected intelligence. 6G will integrate sensing with communication in a single system. Radio waves can be exploited to "see" the physical world and make a digital twin in the cyber world. This paper introduces the concept of integrated sensing and communication (ISAC) and typical use cases, and provides two case studies of how to use 6G ISAC to improve localization accuracy and perform millimeter level imaging using future portable devices. The research challenges to implementing ISAC in practice are discussed.**

II-5.1. Introduction

In 6G mobile communication systems, the use of higher frequency bands (from mmWave up to THz), wider bandwidth, and massive antenna arrays will enable high accuracy and high-resolution sensing, which can help implement the integration of wireless signal sensing and communication (ISAC)[1] in a single system for their mutual benefit. On the one hand, the entire communications network can serve as a sensor. The radio signals transmitted and received by network elements and the radio wave transmissions, reflections, and scattering can be used to sense and better understand the physical world. The capabilities to obtain range, velocity, and angle information from the radio signals can provide a broad range of new services, such as high accuracy localization, gesture capturing and activity recognition, passive object detection and tracking, as well as imaging and environment reconstruction [2]. This is called "network as a sensor". On the other hand, the capabilities of high-accuracy localization, imaging, and environment reconstruction obtained from sensing can improve communication performance.

II-5.2. ISAC use case overview

Wireless sensing has long been a separate technology developed in parallel with the mobile communication systems. Positioning is the only sensing service that mobile communication systems (until 5G) could offer. General sensing rather than positioning will become a new function integrated into the 6G mobile communication system. This capability will open up brand new services for 6G. These services are currently provided by various dedicated sensing equipment, such as radar, light detection and ranging (LIDAR), and professional CT and MRI equipment. The ISAC capability will thus enable many new services that mobile communication system operators can offer. These include very high accuracy positioning, localization and tracking, imaging for biomedical and security applications, simultaneous localization and mapping to automatically construct maps of complex indoor or outdoor environments, pollution or natural disaster monitoring, gesture and activity recognition, flaw and material detection and many other services. These services will in turn enable application scenarios in all kinds of business for future consumers and vertical industries. The potential new services that could be supported by future ISAC systems are listed in Table 1. In the table, the use cases are categorized into four functional categories across different applications/industries (vertical industry, consumer and public services):

- High-accuracy localization and tracking
- Simultaneous imaging, mapping and localization
- Augmented human sensing
- Gesture and activity recognition

II-5.3. ISAC for centimeter-level positioning

The integration of sensing and communication functions can happen at three different levels, from loosely coupled to fully integrated. At the lowest integration level, sensing and communication capabilities can co-exist on hardware by sharing the spectrum, which is more efficient than dedicated spectrum usage. Sensing can benefit from the economies of scale in the mobile communication network, where shared hardware will be cost effective and eases deployment and 6G requires solutions for sub-centimeter level positioning techniques for various future applications and use cases. This level of accuracy for positioning requires much more detailed knowledge of the radio signal propagation environment where sensing comes into play. By learning the environment RF map and the way the transmitted waveform is manipulated by it, the UE position can be obtained as a function of the measurement parameters. This way, the multipath nature of the propagation channel will be helpful. Moving to higher frequencies can further facilitate such sensing-assisted positioning because the channel becomes sparser, and hence, characterizing the mapping between UE position and its propagation channel takes less effort. In a reflection-dominant environment (which is the case in higher frequencies), one such mapping can be obtained by decomposing the multipath channel as multiple LOS channels coming from multiple anchors. Those anchors are obtained by mirroring the transmission point (TP) over the surface of the corresponding reflector for each path. Those virtual anchors are referred to as virtual TPs or vTPs.

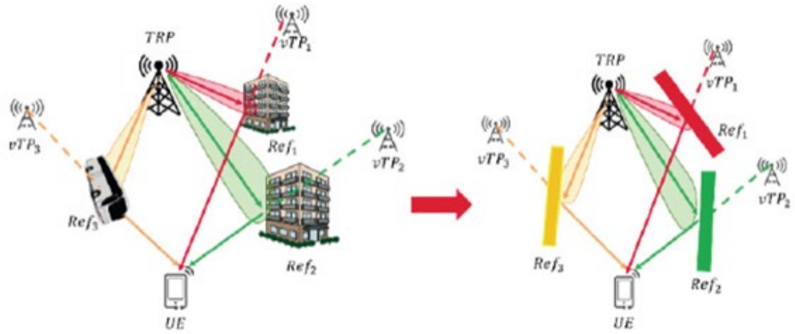

Figure III-5.1 Mapping the objects/reflectors of the environment to virtual anchors, i.e., mapping multipath components to vTPs.

II-5.4. ISAC for mm-level imaging at the THz band

THz lies between the mm-Wave and infrared frequencies, and thus has millimeter-level and even sub-mm level wavelength, making the ISAC system at the THz band (ISAC-THz) particularly suitable for high resolution sensing applications such as millimeter-level resolution 3D imaging. Like the other lower frequency radio waves, THz can penetrate some obstacles, achieving high-precision sensing in all weather and lighting conditions. Recent developments in semiconductor technology have bridged the "THz band gap" and made the hardware feasible at the terminal side. ISAC-THz based portable devices will thus open the door for numerous new sensing applications such as augmented human sensing with very high resolution.

II-5.5. Compressed sensing-based tomography imaging

A major challenge for the virtual aperture imaging technique is the irregular scanning trajectory caused by the user moving the ISAC imaging module to perform THz scanning on an object. Assume a zigzag scanning routine is used to image an object, as shown in A major challenge for the virtual aperture imaging technique is the irregular scanning trajectory caused by the user moving the ISAC imaging module to perform THz scanning on an object. Assume a zigzag scanning routine is used to image an object, as shown in Figure III-5.2. The echo samplings in the horizontal direction are continuous, i.e., the spatial spacing between sampling points is comparable to the wavelength of the echo signal. However, continuous sampling cannot be maintained in the vertical direction. As a result, the echo samplings in the vertical direction are sparse, which will cause high and non-uniform sidelobe effects, giving rise to false artifacts, which may lead to imaging failure. To solve this challenge, we consider decomposing the scanning trajectory on a two-dimensional (2D) plane into several sets of linear scanning tracks along the horizontal direction, where the sparseness of the sampling signals in the vertical domain is then equivalent to the sparseness between horizontal tracks, as illustrated in Figure III-5.2. In this case, the reflected/echo information from the object can be retrieved from these vertically sparse samplings via compressed sensing techniques [3]. As depicted in Figure III-5.3(a), the robotic arm scans at a speed of 1 m/s with the scanning area set as 10 cm by 12 cm in the prototype.

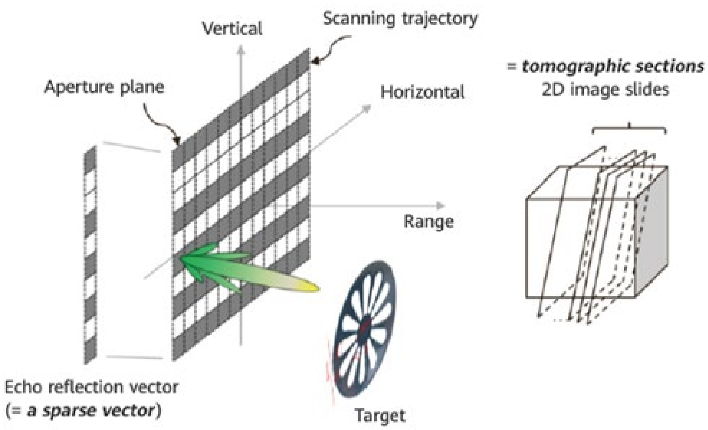

Figure III-5.2 Illustration of the sparse scanning approach and the tomographic imaging techniques.

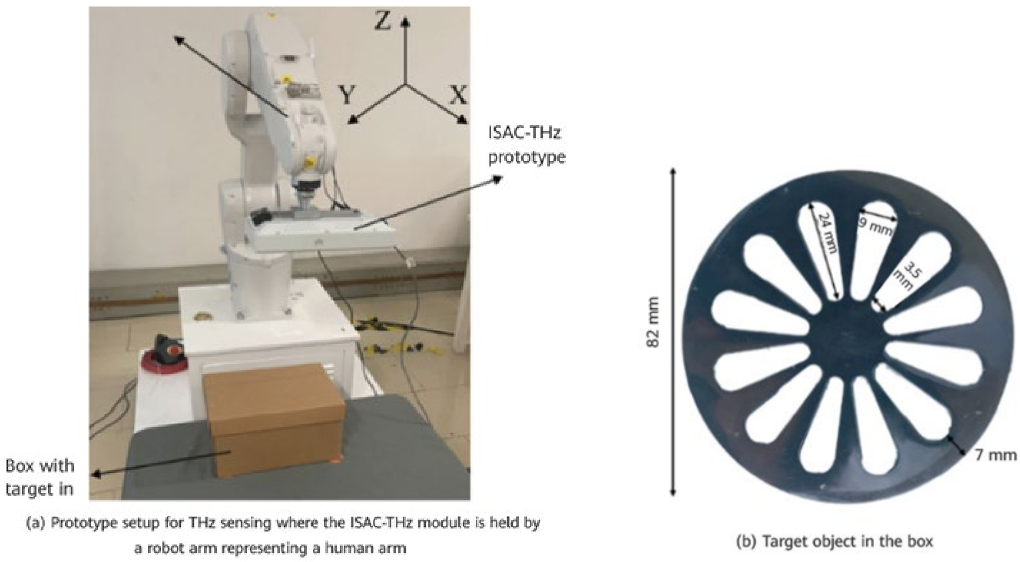

Figure III-5.3 Setup of the ISAC-THz prototype.

The longitudinal spacings of the scan trajectories are controlled to simulate the sparsity in the trajectories of the user's hand-held scanning behavior. The target object to be imaged, as shown in Figure III-5.3 (b), is put in a box with a cap on top of it. As we can see from Figure III-5.3(b), the smallest distance in the hallowed pattern is 3.5 mm, so the highest resolution of the imaging results can be 3.5 mm. The proof-of-concept THz imaging performances with different sparsity configurations in the scanning patterns are presented and compared in Figure III-5.4. In each of the figures, the 3D imaging results are shown on the left and the cross-range profile perceived from top down is shown on the right. The non-sparse full aperture scanning in Figure III-5.4(a) is an ideal case, in which the vertical sampling is half wavelength adjacent. This achieves the best PSLR and ISLR performance, which is set as an upper bound performance reference. Then, in order to simulate the sparsity in real free hand scanning, we assume different sparsity configurations in tests, from 50% (medium sparsity) to 25% (most sparsity), where X% sparsity means that there are X % of the full samplings remaining in the vertical direction. With the collection of fewer samplings, stronger sidelobe interference occurs at the resulted aperture, resulting in worse imaging performance. From the comparison of Figure III-5.4(c) and Figure III-5.4 Figure III-5.4(d), we see that when the sparsity is too high, the traditional tomography algorithm is not enough to recover the images. In this case, the compressed-sensing based tomography approach showed its superior performance.

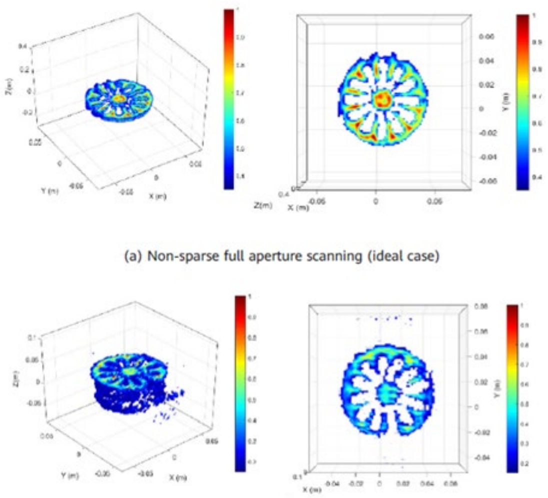

(a) Non-sparse full aperture scanning (ideal case)

(b) Sparse scanning with 50% sparsity (medium sparsity)

Figure III-5.4 Imaging results at different sparsity configurations.

II-5.6. Conclusion

With the concept of ISAC being commonly accepted as one of the key technology trends for 6G, this paper takes a step forward and elaborates two case studies on how 6G ISAC technologies can be applied to improve localization and to perform high resolution imaging. In particular, the proposed SAPE scheme utilizes the joint benefit of device free and device-based sensing and greatly improves the positioning accuracy compared with the current NR scheme. The prototype of the THz camera justifies the feasibility of mm-level imaging resolution on portable devices for both 2D and 3D objects placed in a box. Joint efforts from both academia and industry are needed to address further challenges in the system level evaluation of ISAC, new channel modeling methodology, new waveform design, low complexity algorithm design, and low-cost hardware design.

REFERENCE

[1] Integrated Sensing and Communication (ISAC) – From Concept to Practice,

https://www.huawei.com/en/huaweitech/future-technologies/integrated-sensing-communication-concept-practice
[2] W. Tong, P. Zhu, et al., "6G: the next horizon: from connected people and things to connected intelligence," Cambridge: Cambridge University Press, 2021.
[3] O. Li et al., "Integrated sensing and communication in 6G: a prototype of high-resolution THz sensing on portable device," in European Conference on Networks and Communications (EuCNC), 8-11 June, 2021.

II-6. Space-Time Synchronization

Tetsuya Ido, Nobuyasu Shiga, Motoaki Hara, Yuichiro Yano,
Satoshi Yasuda, Ryuichi Ichikawa
NICT

***Abstract*—For mobile communication technology to transform from a means of man-to-man communication to an infrastructure for various vertical sectors in society, the method of the time synchronization should shift from the traditional leader-follower structure to autonomous distributed synchronization. Furthermore, synchronization must not only be limited to time but also extend to space, entailing the sharing (synchronization) of spatial coordinate axes. This would be realized by three basic technologies, namely compact atomic clocks, wireless time synchronization, and cluster clock systems. The combination will eventually acquire sensing capabilities like distance measurement through radio wave propagation time.**

II-6.1. Introduction

Networks have so far operated under the assumption that participant clocks are not synchronized, establishing a kind of pseudo-synchronization on a one-to-one basis when necessary, where signal transmission time was not taken into account. On the other hand, GNSS has vividly demonstrated its high value by having participants (in this case, many GNSS satellites) with perfectly synchronized clocks, where signal transmission time was taken into account. A prime example is the ability of positioning through radio wave propagation time. Currently, mobile network base stations obtain time from GNSS, but synchronization to GNSS time requires a certain duration, during which the local clock frequency drifts, making it not easy to maintain a consistently synchronized clock in ns level. Additionally, synchronization through GNSS has limitations, such as being unusable indoors and vulnerability due to weak satellite signal strength. Furthermore, we should note that the heavy societal dependence on GNSS has led to considerations for timekeeping methods independent of GNSS, as indicated by executive orders from the United States [1].

Beyond 5G networks are expected to transcend mere human communication and become a social infrastructure for various economic activities. Space-time synchronization proposed here will demonstrate solutions to the concern about the resiliency while enjoying the benefits of a synchronized network. This is based on:

(1) Enhancing the basic strength of synchronized systems by implementing inexpensive, miniaturized atomic clocks in base stations, autonomous vehicles, and even mobile devices in future.

(2) Measuring time differences between clocks at nodes and achieving high-precision synchronization when necessary. Wireless time difference measurement or time synchronization also enables distance measurement based on the signal propagation time.

(3) Creating a virtual clock through the weighted average of local clocks at individual nodes and sharing it across the network, thus generating a standard network clock with high resiliency.

II-6.2. Three technologies comprising space-time synchronization

Toward 6G, ITU-R WP5D composed a document of technology aspects, “Future technology trend for IMT-2030” [2]. This document clearly mentions that the three technologies are key for real-time communications/services. Here, we briefly describe what they are, as follows.

II-6.3. Chip-level integrated frequency standard (CLIFS)

Atomic clocks, with its ticking rate determined by atomic transition frequencies and known for their extremely high frequency stability, became commercially available with the size of a matchbox in 2010. However, mass production was not feasible, limiting their widespread use in consumer products. Recent advances in MEMS technology are about making it possible to mass-produce atomic cells and GHz band oscillators with low phase noise, leading to reduced costs. For instance, Figure III-6.1 shows mass-produced atomic cells using silicon process technology. As a source oscillator, 3.4 GHz oscillator using a solid-state thin-film element (FBAR) recently achieves low phase noise below -124 dBc/Hz at the power consumption of 3mW. The size projected currently ongoing is not yet suitable for handsets but is sufficient for base stations, autonomous vehicles, and drones.

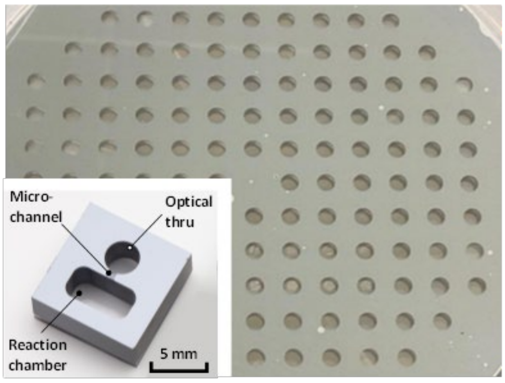

Figure III-6.1 Attempt for mass production of alkali-atom cells using MEMS technology.

II-6.4. Wireless Two-way Interferometry (Wi-Wi)

To achieve high precision in comparing local clock times, signals are sent bidirectionally between nodes, enabling the measurement of both clock difference and signal propagation time. Wireless Two-way Interferometry (Wi-Wi) achieves both syntonization (=identical frequency) and synchronization through the carrier wave of wireless communication. Wi-Wi first compares the carrier phase difference between the local clocks of leader and follower modules. Phase locking (precise syntonization) is accomplished as the follower module stabilizes its local clock to the leader clock. After clock drift is corrected by phase stabilization, the clock is compared through packet transmission and arrival timings. The follower module can then adjust its clock to the leader clock for synchronization.

We have developed a module incorporating a commercial off-the-shelf 920MHz RF chip, fully aligned with the IEEE 802.15.4g standard. It can stabilize the phase with a jitter of ~20 ps and then synchronize the clock to 30 ns. Figure III-6.2 shows the latest version of our Wi-Wi module, where the board size is 67.25mm x 31.75mm.

Two-way measurement provides the significant byproduct of ranging, stemming from the propagation time measurement. Phase measurement allows us to measure distance variation at the sub-cm level. While there is room for improvement in synchronization error, combining it with wide-bandwidth signals can feasibly suppress it to the sub-ns level.

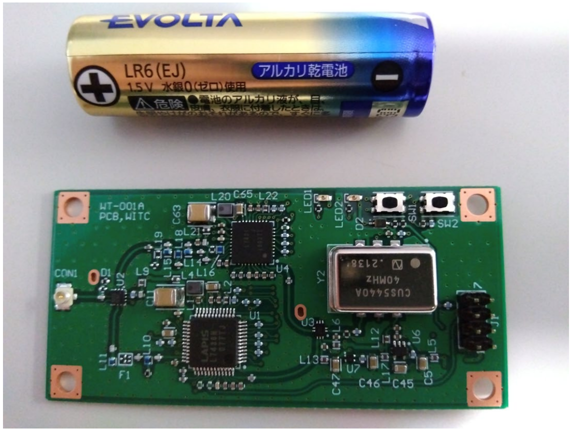

Figure III-6.2 Wi-Wi module.

II-6.5. Cluster clock system

With local clocks having high frequency stability, it may not be the best way to synchronize with an external master clock with a wide servo bandwidth. Rather, making slight frequency adjustments to the atomic clock within a low bandwidth might yield a more stable and reliable clock. Also, creating a virtual clock by locally sharing a weighted mean of the many clocks within the network enhances frequency stability and reduces the risk that specific clock failures affect whole network. Figure III-6.3 shows a POC setup where ten nodes, each equipped with compact atomic clocks, are installed within the same rack and interconnected by optical fiber, realizing a wired cluster clock architecture. A virtual clock is generated through numerical processing from the time difference between the neighbor clocks. Adding frequency and phase offset to the signal of local free-running atomic clocks, each node can generate the ensemble clock as real signals.

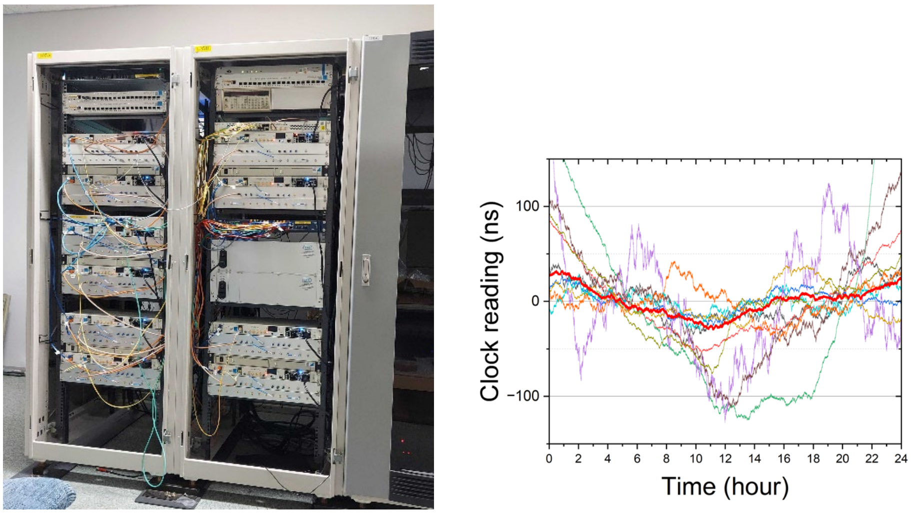

Figure III-6.3 Demonstration of a cluster clock.
Left: Ten nodes equipped with compact atomic clock are connected in a star topology.
Right: Records of clock reading in one day. Cluster clock (red curve) shows an enhanced stability, whereas ten thin curves are those of each clock.

II-6.6. Space-Time Synchronization

Traditionally, synchronization often has involved a leader-follower model where the leader's signal is followed by the followers, including delay as well as noise within the propagation delay, signifying that the time coordinate axis between the leader and follower are not shared. This indicates that synchronization is about sharing the time coordinate axis. Extending this concept to space constitutes the idea of space-time synchronization. Wi-Wi, by measuring propagation delays, enables distance measurements. Furthermore, combining multiple units allows for positioning. This implies that the spatial coordinate axes are shared among network participants, leading to applications like multiple machines coordinating work based on the information of mutual positioning, or multiple vehicles and pedestrians on roads moving coherently to avoid collisions.

II-6.7. Conclusion

The concepts of space-time synchronization and three key technology that realizes space-time synchronization are briefly described. This idea will make the mobile communication system more robust, resilient, and could make energy efficient.

Acknowledgements
This paper includes the results of research and development conducted by the Ministry of Internal Affairs and Communications (MIC) under its ”Research and Development for Expansion of Radio Resources (JPJ000254)” program.

REFERENCE

[1] Strengthening National Resilience Through Responsible Use of Positioning, Navigation, and Timing Services, U. S. Executive order 13905 (2020), https://www.federalregister.gov/documents/2020/02/18/2020-03337/strengthening-national-resilience-through-responsible-use-of-positioning-navigation-and-timing

[2] Future technology trends of terrestrial International Mobile Telecommunications systems towards 2030 and beyond, ITU-R WP5D Rep ITU-R M. 2516-0

II-7. Experimental Evaluation of WLAN-based Device-Free Localization Using CSI in Outdoor and Large-scale Indoor Environments

Osamu MUTA, Shunsuke SHIMIZU
Kyushu University
Tomoki MURAKAMI, Shinya OTSUKI, Hanae OTANI
NTT Corporation

Abstract— **Wireless local area network (WLAN)-based device-free localization techniques using channel state information (CSI) have been investigated, where CSI feedback frames are collected and used as a dataset for machine learning (ML)-based localization. However, CSI-based localization scheme performance depends strongly on radio propagation environments such as the existence of reflective obstacles and WLAN antenna positions. This paper introduces our recent studies with experimentation on WLAN-based device-free localization in outdoor and large-scale indoor environment scenarios. Experiment results confirmed that the developed localization scheme enhances the localization accuracy in specific areas effectively by properly positioning the access point (AP) and the terminal. We also discuss the degree to which performance difference is observed in various scenarios with different AP and terminal positions.**

II-7.2. Introduction

Integrated sensing and communication (ISAC) technologies have been investigated actively as a potential key technology to support 6G networks [1]. Recently, device-free indoor object detection approaches using radio signals of existing communication infrastructure, such as wireless local area networks (WLANs), have attracted much attention [2]–[9], where large amounts of channel state information (CSI) in frequency and spatial domains are acquired simultaneously using multi-input multi-output (MIMO) transmission with orthogonal frequency division multiplexing (OFDM). From several earlier studies [5]–[9], WLAN-based device-free indoor localization schemes have been proposed, where CSI feedback frames (beamforming weights) are collected and used as effective feature data for training machine learning (ML) models and for detecting a target object and its behavior. Based on results of these studies, the developed localization scheme was reported as working well in small-scale indoor scenarios. Nevertheless, the performance achieved in large-scale indoor and outdoor environments has not been clarified.

This paper presents descriptions of our recent studies of WLAN-based device-free indoor localization in outdoor and large-scale indoor experiment scenarios. We demonstrate by experimentation that our developed localization scheme with small datasets enhances the localization accuracy effectively in specific areas by properly positioning the AP antennas and terminals.

II-7.3. WLAN system using CSI-based localization approaches

Figure III-7.1 presents principles of CSI acquisition for a device-free WLAN-based localization consisting of an access point (AP), a station (STA), and a CSI- acquisition terminal, where M, N, and S respectively denote the numbers of transmit antennas, received antennas, and streams. Here, a single target is present within an observation area. The principle of device-free localization is identification of the target object behavior through variations in wireless channel characteristics, as shown in frequency-domain CSI of this figure. Consequently, target detection is expected to be achieved by learning the relation between the states of the target and of the wireless channel without requiring that the target have any wireless device. A challenging issue is acquisition of a sufficient amount of CSI from an environment. An effective method is to use CSI in existing IEEE802.11-based WLAN systems. On the STA side, after channel estimation, a compressed version of a right-singular matrix obtained by singular value decomposition of the channel matrix is fed back to the AP side as beam-forming weights (BFWs).

Figure III-7.2 portrays a block diagram of CSI acquisition terminal that collects feedback frames sent by the STA. To improve the localization performance, an effective lightweight algorithm with a small dataset [6]–[9] is adopted, where current and past BFWs are concatenated as single data to build more accurate feature data. After concatenating multiple BFWs as single feature data, they are used both for off-line training and for on-line detection.

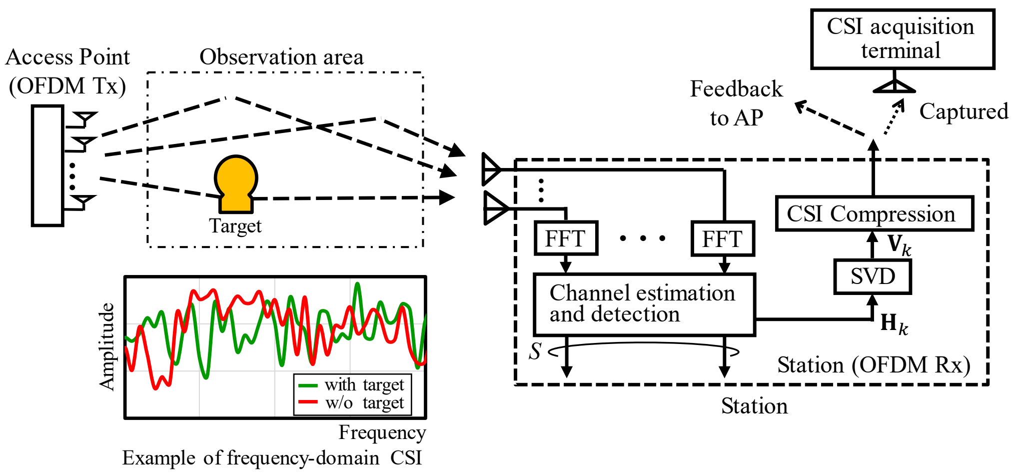

Figure III-7.1 Principles of CSI acquisition for WLAN-based device-free localization.

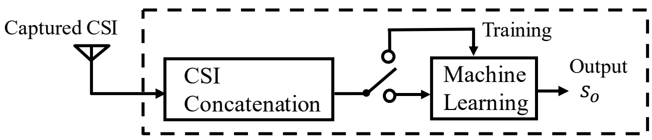

Figure III-7.2 Block diagram of the CSI acquisition terminal.

II-7.4. Experiment scenario and results

To demonstrate the effectiveness of the developed algorithm in various environments, we conducted evaluations of our developed localization scheme by experimentation in outdoor and large-scale indoor scenarios using an IEEE802.11ac-based WLAN [10]. The experiment scenario and setup are depicted in Figure III-7.3. As typical scenarios with few nearby reflective objects, we conducted experiments in an outdoor place and a gymnasium on our university campus as shown respectively in Figure III-7.3(a) and Figure III-7.3(b). Here, photographs of the experiment environments are also presented. In these figures, the observation areas are represented by the red-shaded area enclosed by the red dashed line. Experiment details are presented in an earlier report [9]. The coverage area in Figure III-7.3(c) is segmented into Q regions (areas), denoted as q = 1, … , Q, where Q is set as 20. For this experiment, we approach it as a multi-class classification problem to identify the location (label) of a single target object. The AP has four antennas connected by a coaxial cable. The STA is mounted on a tripod. The CSI feedback frames, which serve as the dataset, are collected at the CSI acquisition terminal. Random Forest model is used and built at the CSI acquisition terminal by off-line training with measured CSI. We evaluate the detection probability, which is defined as a conditional probability that the ML result is the same as the actual label number, where a target person is within one of the Q=20 labeled areas.

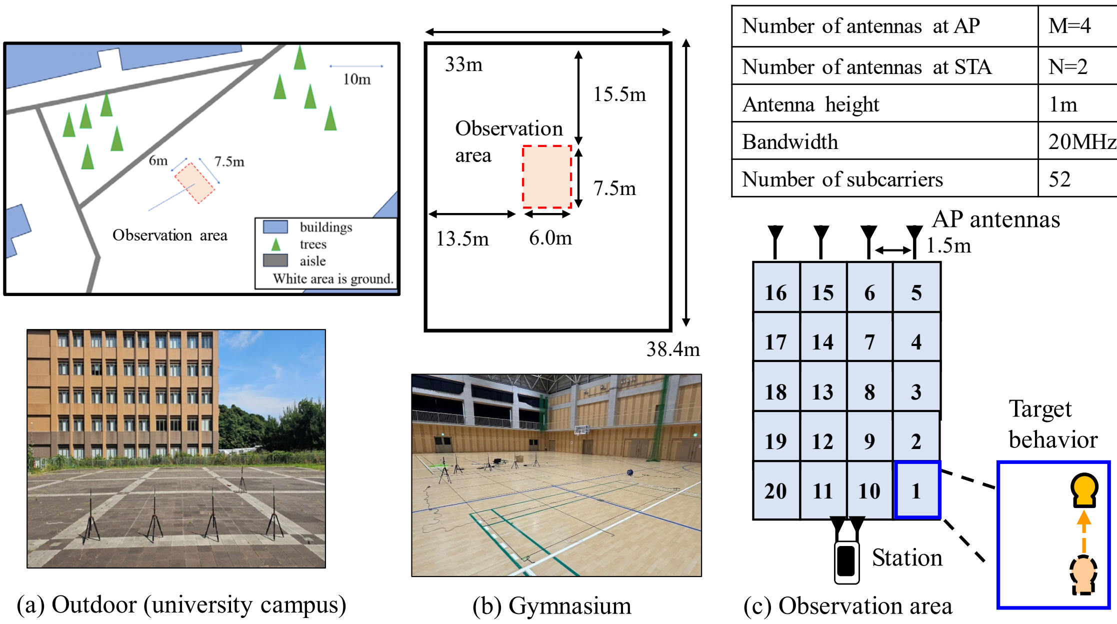

Number of antennas at AP	M=4
Number of antennas at STA	N=2
Antenna height	1m
Bandwidth	20MHz
Number of subcarriers	52

Figure III-7.3 Experiment scenario and setup [9].

Figure III-7.4 presents the average area-wise detection probability (heatmaps) for outdoor experiment scenarios using different STA positions, where the experiment setup is the same as in Figure III-7.3(a). Here, green circles represent the positions of the AP antennas, whereas blue circles represent the STA positions. The heatmap intensity corresponds to the detection probability in each labeled area. Results show that areas directly facing the AP and STAs have higher detection probability, whereas other areas experience a marked drop in detection probability. This finding suggests that strategic placement of AP antennas and STAs can enhance detection probability intentionally in specific areas.

Figure III-7.5(a) and Figure III-7.5(b) show average area-wise detection probability (heatmaps) in a large-scale indoor environment (gymnasium in Figure III-7.3(b)) for different STA positions. Results indicate that the area-wise detection probability has a similar tendency to that of outdoor scenarios in Figure III-7.4. Panel (c) presents the average detection probabilities of cover areas and the other areas, defined respectively as orange-colored (labels 5–16) and yellow-colored areas (labels 1–4 and 17–20). The findings confirm that much higher detection probability is achieved in cover areas where AP and STA are faced, than in the other areas.

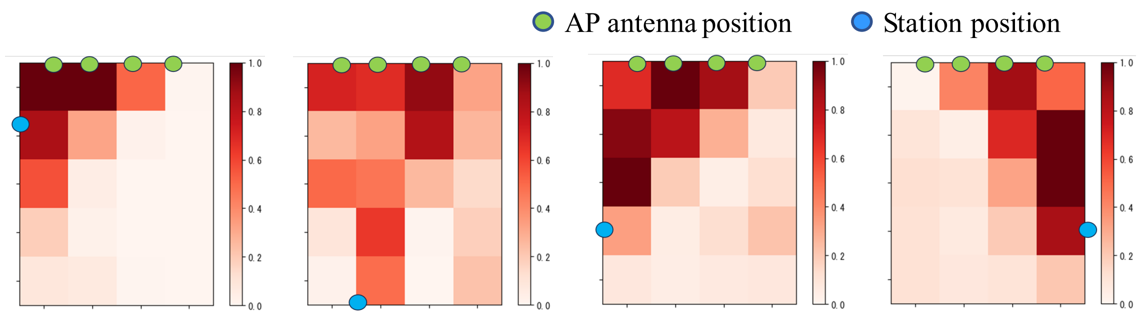

(a) Scenario 1-1 (b) Scenario 1-2 (c) Scenario 1-3 (d) Scenario 1-4

Figure III-7.4 Area-wise detection probability (heatmap) for outdoor experiment scenarios using different STA positions [9].

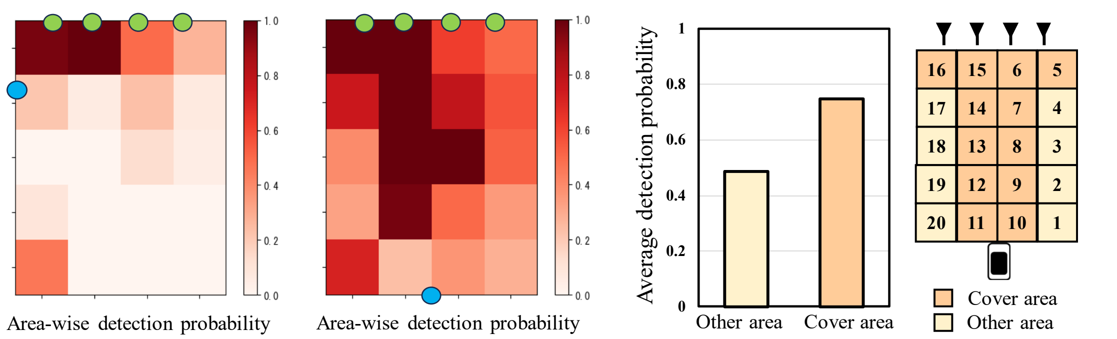

(a) Area-wise detection probability (heatmap) (b) Average detection probability for cover and other area

Figure III-7.5 Average detection probability for large-scale indoor experiment scenario [9].

II-7.5. Conclusion

This report describes experiment-based evaluation and the achieved localization performance of a WLAN-based localization scheme with a small dataset in outdoor and large-scale indoor environments. The experimentally obtained results demonstrated that the detection probability can be enhanced effectively in specific locations by appropriately setting the AP and STA locations. Developing object detection algorithms for various use cases is left as a subject for our future work.

Acknowledgements

We thank Mr. Fuma Kunihiro, a student of Kyushu University, for their contributions to this research.

REFERENCE

[1] "White Paper 5G Evolution and 6G (Version 5)," NTT DOCOMO, Inc., Jan. 2023.

[2] A. Behravan, V. Yajnanarayana, M.F. Keskin, H. Chen, D. Shrestha, T.E. Abrudan, T. Svensson, K. Schindhelm, A. Wolfgang, S. Lindberg, and H. Wymeersch, "Positioning and sensing in 6G gaps, challenges, and opportunities," IEEE Veh. Technol. Mag., vol. 18, no. 1, pp. 40–48, Jan. 2023.

[3] H. Jiang, C. Cai, X. Ma, Y. Yang, and J. Liu, "Smart Home Based on WiFi Sensing: A Survey," IEEE Access, vol. 6, pp. 13317–13325, March 2018.

[4] H. Zhu, F. Xiao, L. Sun, R. Wang, and P. Yang, "R-TTWD: Robust Device-free Through-the-wall Detection of Moving Human with WiFi," IEEE Journal on Selected Areas in Communications, vol. 35, no. 5, pp. 1090–1103, March 2017.

[5] T. Murakami, M. Miyazaki, M. Ishida, and A. Fukuda, "Wireless LAN Based CSI Monitoring System for Object Detection," MDPI Electronics, Nov. 2018.

[6] O. Muta, K. Takata, K. Noguchi, T. Murakami, and S. Otsuki, "Device-Free WLAN Based Indoor Localization Scheme with Spatially Concatenated CSI and Distributed Antennas," IEEE Trans. Vehicular Technology, vol. 72, no. 1, pp. 852–865, Jan. 2023.

[7] O. Muta, K. Noguchi, J. Izumi, S. Shimizu, T. Murakami, and S. Ohtsuki, "Device-free Indoor WLAN Localization with Distributed Antenna Placement Optimization and Spatially Localized Regression," IEEE Trans. Wireless Commun., vol. 23, issue 8, pp. 9869–9883, Aug. 2024.

[8] O. Muta, J. Izumi, S. Shimizu, T. Murakami, and S. Otsuki, "Experimental Evaluation of Device-free Indoor Localization Using Channel State Information in WLAN Systems with Distributed Antennas," IEICE Trans. Commun., vol. E107-B, no. 12, pp. 890–898, Dec. 2024.

[9] S. Shimizu, O. Muta, S. Otsuki, T. Murakami, and H. Otani, "Experimental Evaluation of WLAN-based Object Detection Using CSI in Outdoor and Large-scale Indoor Environments," IEEE Vehicular Technology Conference Fall 2024, Oct. 2024.

[10] IEEE Computer Society, IEEE 802.11-2016, LAN/MAN Standards Committee, 2016.

II-8. A Fundamental Study on the Relationship Between Pedestrian Traffic and Wi-Fi CSI with Existing Outdoor Access Points

Masakatsu Ogawa, Sophia University

Abstract— **This paper describes the relationship between pedestrian traffic and Wi-Fi channel state information (CSI) with existing outdoor access points (APs). Conducted on a university's main street, pedestrian traffic was measured using YOLOv8, and CSI variation was analyzed. The results show a correlation between CSI variation and congestion conditions, demonstrating the feasibility of estimating pedestrian traffic using CSI variation from existing Wi-Fi APs.**

II-8.2. Introduction

Currently, Wi-Fi access points (APs) are deployed in various locations, such as homes, offices, schools, and public spaces. The primary role of Wi-Fi is to transmit and receive traffic between AP and stations (STAs). Additionally, APs broadcast network information through beacon frames. In the 5GHz band, beacon frames are transmitted using orthogonal frequency division multiplexing (OFDM) signals, as specified in the IEEE 802.11a standard. Therefore, channel state information (CSI), which represents frequency-domain characteristics, can be extracted from beacon frames.

In schools and public spaces, APs are often deployed outdoors. CSI is expected to be useful for estimating outdoor conditions, such as pedestrian and vehicle traffic on roads.

Until now, most studies on Wi-Fi CSI have focused on indoor environments, requiring users to deploy APs themselves. This paper addresses leveraging existing outdoor Wi-Fi APs to estimate pedestrian traffic on roads. This paper reports a fundamental study on the relationship between pedestrian traffic and Wi-Fi CSI using existing outdoor access points [1].

II-8.3. Measurement Setup

Sophia University has deployed Wi-Fi APs both indoors and outdoors. The university's main street is within the Wi-Fi coverage area. On class days, this street is crowded during break times, relatively clear during class times, and nearly empty during gate closing times. Therefore, pedestrian traffic changes from time to time.

Figure III-8.1 displays the university's main street, captured by a camera for measuring pedestrian traffic. University Wi-Fi APs have been installed facing the main street, and one AP is selected based on the camera image. The four receiving antennas for acquiring CSI are installed in the same building as the university's Wi-Fi APs. CSI is measured using one of the four receiving antennas. Since the beacon interval is 100 ms, the CSI measurement interval is also 100 ms. When pedestrians walk through the measurement area, CSI fluctuates due to multipath reflections. Pedestrian traffic is measured using YOLOv8, an object detection algorithm. The measurement area is indicated by the red line in Figure III-8.1.

Figure III-8.1 Measurement environment.
Left: Locations of measurement equipment. Right: Measurement area.

II-8.4. CSI variation

The CSI variation is derived from the moving variance of CSI amplitude components [1]. Since beacon frames are transmitted by a single antenna, CSI is measured separately by each receiving antenna. Let k be the subcarrier index, and t the beacon frame index. Each element $h_{m,k,t}$ of the CSI matrix is expressed as a complex number, as shown in Equation (1). In the IEEE 802.11a standard, the number of data subcarriers is 48.

$$h_{k,t} = |h_{k,t}| e^{j\angle h_{k,t}} \tag{1}$$

The time-series data of CSI amplitude, H_t, at time t is defined in Equation (2).

$$H_t = [|h_{1,t}|, |h_{2,t}|, \dots, |h_{k,t}|, \dots, |h_{48,t}|] \tag{2}$$

To focus on the fluctuation of each subcarrier, the H_t is normalized using the norm of H_t, $\|H_t\|$. The normalized time-series data of CSI amplitude, $\widehat{H}_t$, is expressed in Equation (3).

$$\widehat{H}_t = \left[\frac{|h_{1,t}|}{\|H_t\|}, \frac{|h_{2,t}|}{\|H_t\|}, \dots, \frac{|h_{k,t}|}{\|H_t\|}, \dots, \frac{|h_{48,t}|}{\|H_t\|}\right] \tag{3}$$

Let tw be the time window for the moving variance. The normalized time-series data of CSI amplitude within this time window at time t, $\widehat{TH}_{k,t}$, is given in Equation (4).

$$\widehat{TH}_{k,t} = [\widehat{H}_{t-tw+1}^T, \dots, \widehat{H}_t^T] \tag{4}$$

The sum of the variance of $\widehat{TH}_{k,t}$ for each subcarrier is defined as CSI variation. The time series of CSI variation is obtained using a window shift.

II-8.5. Evaluations

To clarify the relationship between pedestrian traffic and CSI variation, these characteristics are illustrated in Figure III-8.2. Pedestrians within this area are counted every ten seconds over a one-minute period. Similarly, for CSI variation calculation, the time window is set to one minute, with a window shift of ten seconds. To eliminate environmental noise, the Hampel filter is applied to the CSI amplitude component of each subcarrier and the calculated CSI variation.

In this figure, the gate closing time is from 22:00 to 8:00, and the gray hashed areas represent class times. Obviously, pedestrian traffic increases before and after class times. Additionally, CSI variation also increase, and both characteristics exhibit similar trends. The CSI variation does not approach zero around 23:00, likely due to trees swaying in the wind. Except for this anomaly, these characteristics are correlated, allowing congestion status to be estimated using CSI variation.

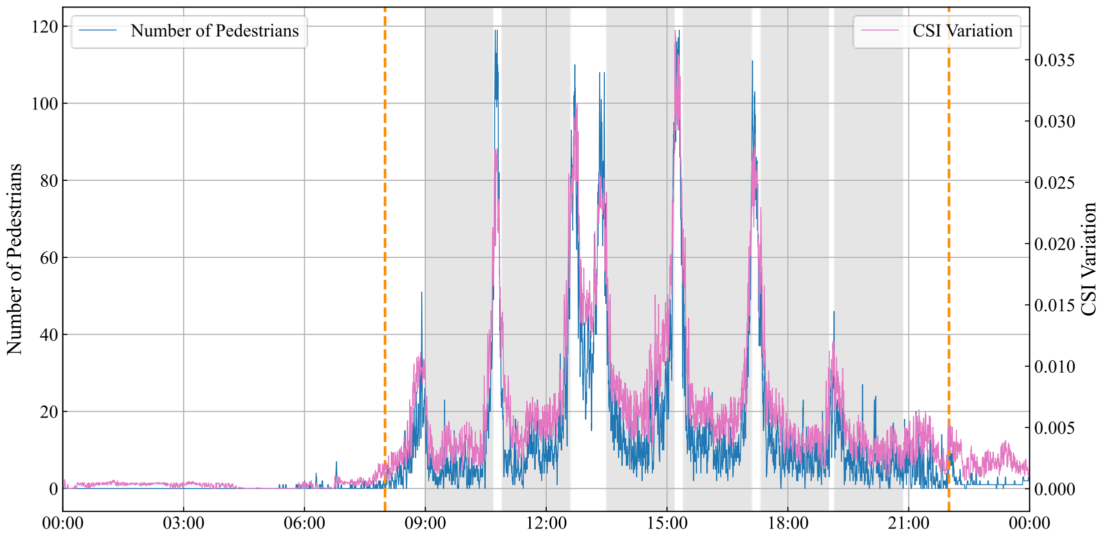

Figure III-8.2 Number of pedestrians and CSI variation.

II-8.6. Conclusion

This paper described the relationship between pedestrian traffic and Wi-Fi CSI with existing outdoor APs. Showed that CSI is closely linked to congestion conditions. The results indicated the feasibility of estimating pedestrian traffic using existing APs without the need for the installation of new APs.

Acknowledgements

This work was supported by JSPS KAKENHI Grant Number 22K12016.

REFERENCE

[1] Keita Tajima, Masakatsu Ogawa, “A Study on Outdoor Pedestrian Traffic Estimation Using CSI in University Wi-Fi,” IEICE Tech. Rep., vol. 124, no. 353, SeMI2024-70, pp. 47-52, Jan. 2025 (Japanese).

II-9. Multipath-RTI: Millimeter-Wave Radio Based Device-Free Localization

Minseok Kim
Niigata University

Abstract— **This paper developed Multipath-RTI, a novel radio tomographic imaging (RTI) method utilizing millimeter-wave (mmWave) signals for device-free localization (DFL). Unlike conventional RTI approaches that struggle with multipath fading and require many physical anchor nodes, Multipath-RTI leverages virtual anchor nodes formed by multipath reflections. The study introduces compressed sensing-based image reconstruction, automatic parameter tuning, and DBSCAN clustering for multi-target location estimation. Results from simulations and mmWave channel sounding measurements show sub-0.5 m accuracy in complex indoor environments.**

II-9.1. Introduction

Indoor localization and position estimation have gained significant interest [1], [2]. While traditional methods based on time-of-arrival or RSS from emitter devices exist, their performance often degrades in real multipath environments. In smart homes and buildings, device-free localization (DFL) is increasingly preferred due to its non-intrusive nature. DFL is especially useful for daily applications like elderly or patient monitoring, and even for identifying individuals in security-critical scenarios where cameras may not be effective.

Radio tomographic imaging (RTI) maps signal attenuation caused by target-induced shadowing using dense RF sensor networks [1]. The area is divided into 2D voxels, whose values are estimated from RSS measurements via an ill-posed inverse problem. In [1], a simple model assumes RSS is a weighted sum of voxel contributions along Line-of-sight (LoS) paths. However, in narrowband systems like ZigBee or Wi-Fi, multipath fading degrades RSS accuracy, requiring many anchor nodes for adequate resolution. While some works have improved narrowband RTI, few have explored multipath-assisted RTI [2]. For example, Cimdins et al. achieved sub-meter accuracy using MPCs from ultra-wideband CIRs, though accuracy dropped near anchors and multi-target cases remain unaddressed.

To address these challenges, the author proposed Multipath-RTI as shown in Figure III-9.1 [3], an RTI method leveraging mmWave radios (e.g., 5G, WiGig) for high-resolution channel acquisition. This enables individual multipath component (MPC) tracking and the use of virtual anchor nodes. However, accurate multipath separation, MPC clustering, and path identification remain difficult. This paper introduces advanced signal processing techniques—compressed sensing, cross-validated parameter tuning, DBSCAN-based multi-target estimation, and ray-tracing-assisted MPC association—validated through double-directional mmWave measurements and simulations.

II-9.2. Multipath-RTI Technique

The target area is divided into a grid of 2D voxels. The received signal strength (RSS) variations are modeled as $\Delta \boldsymbol{y}(t) = \boldsymbol{W}\Delta \boldsymbol{x}(t) + \boldsymbol{n}(t)$, where W is a weight matrix encoding the contribution of each voxel to each multipath component (Figure III-9.2). Here, multipath paths including LoS, single-bounce, and double-bounce links are utilized. A sparse representation is obtained using compressed sensing techniques, solving an ill-posed inverse problem. The voxel values (Δx) are estimated using Elastic Net regularization [4], [5], balancing sparsity and stability.

After estimating voxel values, the RTI image is post-processed using Otsu's binarization to remove artifacts, followed by DBSCAN clustering to estimate the number and locations of targets (Figure III-9.3). This method does not require prior knowledge of target count. Regularization parameters are tuned via cross-validation to optimize the trade-off between noise suppression and spatial accuracy.

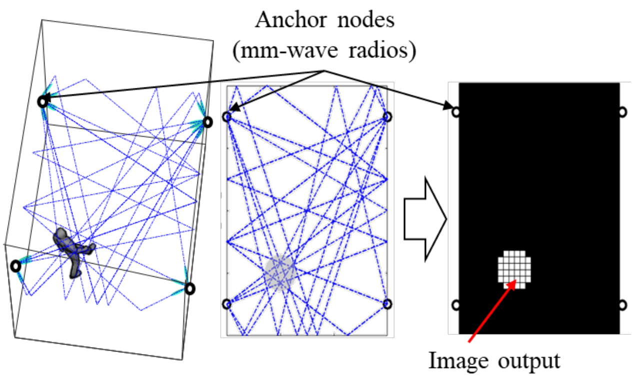

Figure III-9.1 Multipath-RTI technique.

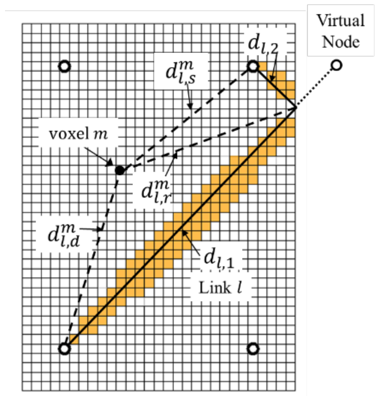

Figure III-9.2 Weight matrix.

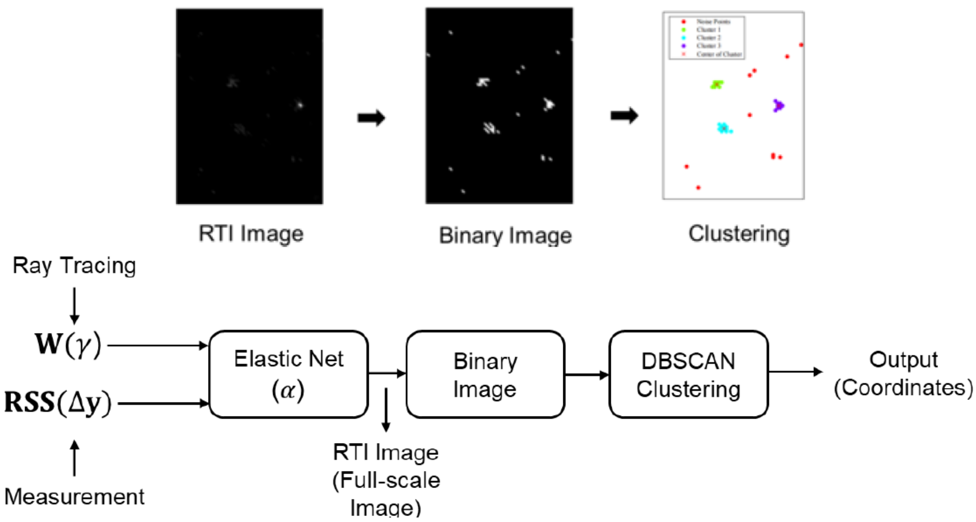

Figure III-9.3 Signal processing.

II-9.3. Performance evaluation

For real-world experiments, the proposed method was developed using a 60 GHz double-directional mmWave channel sounder. The channel sounder consists of in-house baseband units and COTS phased-array transceivers (EVK06002, Sivers IMA) using 16-element ULAs for beamforming. Operating at 58.32 GHz (WiGig CH1), it delivers 31 dBm EIRP with 19 dBi total gain. The azimuth beamwidth is ~6°, with elevation HPBW of 18° (Rx) and 45° (Tx). Beam steering from −45° to 45° allows 90° coverage via 12 beams; four array orientations extend this to 360° with 48 beams. A 4×4 MIMO TDM scheme captures 16 channels per sweep, enabling fast double-directional channel measurements. Ray tracing generates expected path parameters, and a sub-grid CLEAN algorithm extracts MPCs [6].

To validate the DFL capability, mmWave double-directional channel measurements were conducted in an empty room (Figure III-9.4(a)), with anchor nodes placed at positions A–D. Due to hardware constraints, six Tx–Rx links were measured individually using a single Tx/Rx pair mounted at 1.3 m height. Measurements were taken under six conditions: Pos0 (no person) and Pos1–Pos5 (with a person). In post-processing, over 100 multipath components (MPCs) were extracted per link using a high-resolution algorithm [6]. Path association identified 47 valid paths—including LoS, single-bounce, and double-bounce reflections—suitable for Multipath-RTI. Figure III-9.4(b) shows the resulting RTI images. Yellow '×' markers denote estimated target centroids. Results indicate that RTI accuracy improves when more paths are blocked by the target. In positions with limited path obstruction (e.g., Pos4), the target blobs are smaller and more diffuse. Although measurement errors are generally higher than in simulation, all remain below 0.5 m. Optimal parameters depend on factors like room geometry, anchor configuration, and target distribution. Further simulations in L-shaped and obstacle-rich rooms show 88–96% sub-0.5 m accuracy using only 4–8 anchors.

Performance was evaluated for 1–5 randomly placed targets. As target count increased, estimation error and failure rate also rose, especially when targets were close. The OSPA metric and failure analysis indicated a need for temporal filtering. Nevertheless, Multipath-RTI showed resilience by localizing multiple targets using clustering, without needing time-series tracking.

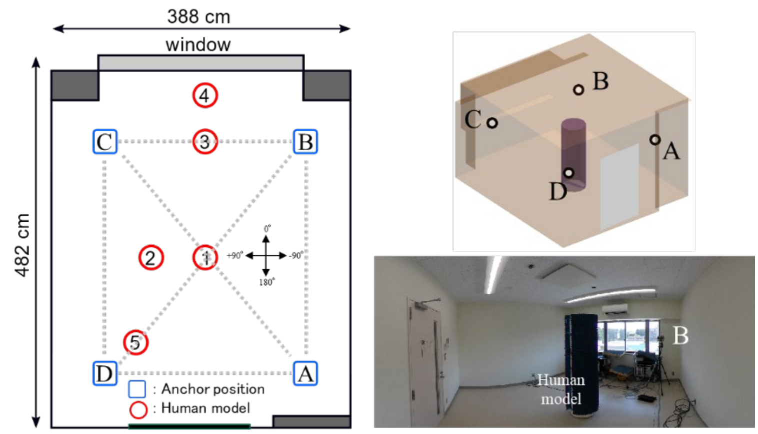

(a) Measurement setup

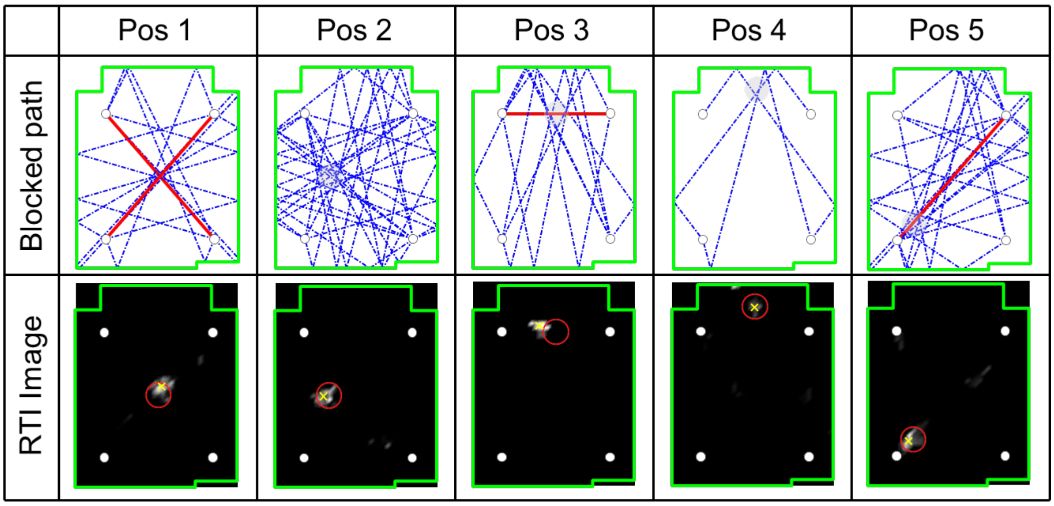

(b) Localization results

Figure III-9.4 Measurement and evaluation.

II-9.4. Conclusion

This paper proposed a signal processing framework for Multipath-RTI using Elastic Net regularization and DBSCAN clustering for accurate, device-free localization. A ray-tracing-assisted method was introduced to associate multipath components, validated through mmWave measurements and simulations. Results showed sub-meter accuracy for both single and multiple targets. However, performance depends heavily on parameter tuning and anchor placement. Future work should address automated optimization, deployment strategies, and system scalability for real-time applications.

REFERENCE

[1] J. Wilson and N. Patwari, “Radio tomographic imaging with wireless networks,” IEEE Trans. Mobile Comput., vol. 9, no. 5, pp. 621–632, May 2010.

[2] M. Cimdins et al., “MA-RTI: Design and evaluation of a real-world multipath-assisted device-free localization system,” Sensors, vol. 23, no. 4, 2023.
[3] T. Ikegami, M. Kim, Y. Miyake and H. Tsukada, "Multipath-RTI: Millimeter-Wave Radio Based Device-Free Localization," IEEE Access, vol. 12, pp. 42042-42054, 2024.
[4] R. Tibshirani, “Regression shrinkage and selection via the lasso,” J. Roy. Stat. Soc., Series B, vol. 58, no. 1, pp. 267–288, 1996.
[5] H. Zou and T. Hastie, “Regularization and variable selection via the elastic net,” J. Roy. Stat. Soc., Series B, vol. 67, no. 2, pp. 301–320, 2005.
[6] M. Kim, T. Iwata, S. Sasaki, J. Takada, “Millimeter-Wave Radio Channel Characterization using Multi-Dimensional Sub-Grid CLEAN Algorithm,” IEICE Trans. Commun.,Vol.E103-B, No.7, pp.767-779, Jul. 2020.

II-10. Verification in an Anechoic Chamber toward the Realization of a Radio Wave Camera Using a Mobile Communication System

Kazuma Tomimoto, Tomonori Ikeda, Ryo Yamaguchi,
Toshiki Hozen, Syumpei Tabuchi,
SoftBank Corp. Research Institute of Advanced Technology

II-10.1. Introduction

Methods for increasing the capacity of mobile communication systems and methods for increasing the accuracy of sensing (radar) have many points in common, and the integration of wireless communication and sensing (ISAC: Integrated Sensing and Communication) is a major pillar of 6th generation mobile communications (6G) [1].

In this paper, in order to perform sensing without significantly disrupting the frame format of 3GPP-compliant signals, the 5GNR downlink signal reflected from a target is received by a virtual array antenna, and the reference signal demodulation and direction estimation algorithms are applied. This result shows that it is possible to estimate the direction of a target by utilizing the reference signal contained in the 5GNR downlink signal.

II-10.2. Measurement Flow

Figure III-10.1 shows the measurement system configuration. Table III-10.1 shows the measurement specifications. The measurement consists of two steps: measurement at actual wave sources and off-line SSB demodulation and array signal processing.

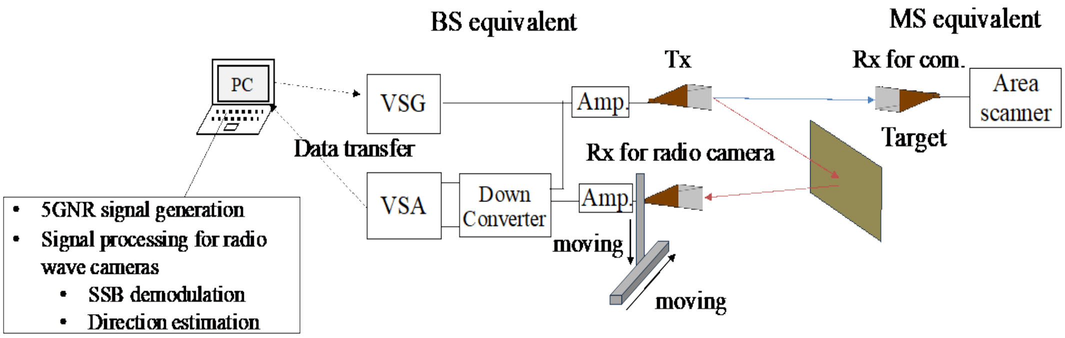

Figure III-10.1 Measurement system configuration.

Table III-10.1 Publication summary of use case in ISAC.

Transmitted signal specifications		Array antenna specifications	
Signal	5GNR FR2	Number of element	20 by 20
Center Frequency	29.3 GHz	Element spacing	0.5 λ
Subcarrier spacing	120 kHz	Tx/Rx	Horn antenna
SSB bandwidth	28.8 MHz	Antenna height	1.3 m

II-10.2.1. Measurement at actual wave sources

Assuming sensing (radar) at the base station side, an Rx for a radio wave camera is installed near the Tx. The Tx for the radio wave camera is a single element, and it transmits 5GNR signals according to the parameters in Table III-10.1.

The Rx for the radio wave camera receives signals while the antenna is moved by a positioner, and a virtual planar array antenna is configured to acquire receiving characteristics. In the actual measurement, there is a possibility that the measurement accuracy will be degraded due to the signal transmitted from the Tx going around the Rx for the radio wave camera. Referring to [2], to eliminate this effect, the receiving characteristics with and without the target installed are measured. Assuming communication between the base station and the mobile station, the Rx for communication is placed at a distance of about 5 m from the Tx. The area scanner connected to the Rx for communication is used to measure the receiving characteristics.

II-10.2.2. Off-line SSB demodulation and direction estimation algorithm

The 5GNR demodulation process is performed on the receiving characteristics obtained in 2.1. From this, the receiving characteristics after the demodulation without target installation $\boldsymbol{H}_{\mathrm{ref}}(k,l)$ and after the demodulation with target installation $\boldsymbol{H}_{\mathrm{meas}}(k,l)$ are obtained. Where k is the subcarrier number and l is the OFDM symbol number. Then, OFDM symbols containing the 5GNR reference signal SSB (SS/PBCH Block) are extracted and $\boldsymbol{H}_{\mathrm{meas}}(k,l)$ is subtracted from $\boldsymbol{H}_{\mathrm{ref}}(k,l)$ to obtain the response from the target, $\boldsymbol{H}(k)$.

The correlation matrix R_{R} is calculated using $\boldsymbol{H}(k)$, and the Beamformer method in eq. (1) is applied to R_{R}. As a result, an angular spectrum of the vertical direction θ and the horizontal direction ϕ is obtained. λ, $\boldsymbol{r}_{n_y n_z}$, $E[\cdot]$,$\{\cdot\}^H$, and $\boldsymbol{a}(\theta,\phi)$ are the wavelength, position vector of the virtual planar array antenna's element, ensemble mean, Hermite transpose, and mode vector.

$$E_{\mathrm{BF}}(\theta,\phi) = \boldsymbol{a}(\theta,\phi)^H \cdot R_{\mathrm{R}} \cdot \boldsymbol{a}(\theta,\phi)/2 \quad (1)$$

$$R_{\mathrm{R}} = E[\boldsymbol{H}(k)\boldsymbol{H}(k)^{\boldsymbol{H}}] \quad (2)$$

$$\boldsymbol{a}(\theta,\phi) = \exp(j\boldsymbol{r}_{n_y n_z} \cdot \boldsymbol{R}(\theta,\phi)) \quad (3)$$

$$\boldsymbol{R}(\theta,\phi) = \frac{2\pi}{\lambda}(\sin\theta\cos\phi, \sin\theta\sin\phi, \cos\theta) \quad (4)$$

II-10.3. Measurement results

Figure III-10.2 shows the measurement scene and results of the area scanner, and Figure III-10.3 shows the direction estimation result.

The measurement system shown in Figure III-10.1 was configured in an anechoic chamber, and a target was actually set up for measurement. Figure III-10.2 shows that the physical cell ID (PCI) of the area scanner is 1, which is the same value as the set PCI. This shows that the signal is transmitted from

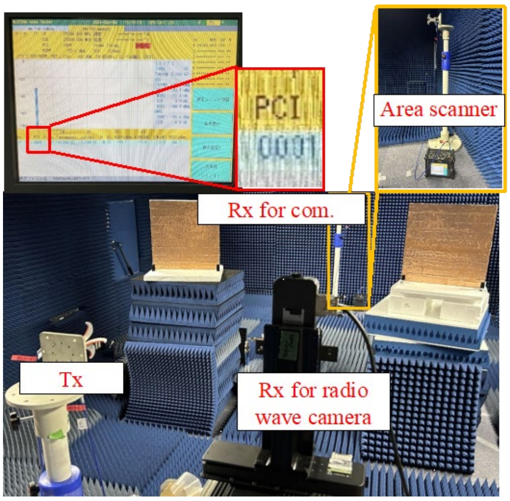

Figure III-10.2 Measurement scene and result of the area scanner.

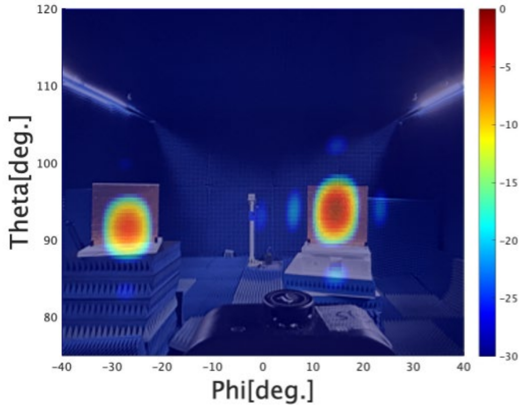

Figure III-10.3 Direction estimation result.

the Tx in compliance with the 5GNR frame format. Next, Figure III-10.3 shows a strong peak of spectrum at almost the same angle as that at which the target was placed. From this result, it was confirmed that the estimation of target direction is possible by using the reference signal included in the 5GNR downlink signal.

II-10.4. Summary and future work

This paper conducted a basic verification of estimation of target direction using reference signals included in 5GNR downlink signals and confirmed its effectiveness. In the future, we will study to enhance target classification and estimation the use of polarization technology, and the use of machine learning.

REFERENCE

[1] Z. Wei, et al. IEEE Internet of Things, vol.10, no.13, pp. 11068-11092, July 2023.
[2] H. Yamamoto et al, IEICE Tech. Rep, vol. 123, no. 336, AP2023-182, pp. 122-125, jan.2024.
[3] N. Kikuma ,“Adaptive Antenna Technology(in Japanese),” Ohmsha, Ltd., Oct. 2003.

Abbreviation List

Abbreviation	Explanation
ABG	Alpha-Beta-Gamma
AI	Artificial Intelligence
ALD	Atomic Layer Deposited
AMC	Adaptive Modulation and Coding
AoA	Angle of Arrival
AR	Augmented Reality
ASIC	Application Specific Integrated Circuit
AWG	Arbitrary Waveform Generator
BAN	Body Area Network
BCB	Benzo cyclobutene
BER	Bit Error Rate
BF	BeamForming
BS	Base Station
CC	Component Carrier
CI	Close-in
CMOS	Complementary Metal Oxide Semiconductor
CPS	Cyber Physical System
CSI	Channel State Information
DC	Direct Current
DFT	Discrete Fourier Transform
DL	Down Link
DNN	Deep Neural Network
DOA	Direction of Arrival
DSP	Digital Signal Processing
EIRP	Effective Isotropic Radiated Power
EVM	Error Vector Magnitude
eWLB	embedded Wafer Level Ball grid array
FDD	Frequency Division Duplex
FDE	Frequency Domain Equalize

Abbreviation	Explanation
FSPL	Free Space Path Loss
HARQ	Hybrid Automatic Repeat Request
HPBW	Half Power Beam Width
IBO	Input Back Off
IFFT	Inverse Fast Fourier Transform
InH	Indoor hotspot cell
ISAC	Integrated Sensing and Communication
ITU-R	International Telecommunication Union Radiocommunication Sector
KPI	Key Performance Indicator
LAN	Local Area Network
LNA	Low-Noise Amplifier
LOS	Light of Sight
LTE	Long Tern Evolution
MCM	Multichip Module
MIMO	Multiple-Input and Multiple-Output
MMIC	Monolithic Microwave IC
MS	Mobile Station
MOS	Metal Oxide Semiconductor
MOS-HEMT	Metal-Oxide-Semiconductor Eigh-Electron-Mobility Transistor
MSL	Microstrip Line
NLOS	Non-Line of Sight
NR	New Radio
NRNT	New Radio Network Topology
OAM	Orbital Angular Momentum
OFDM	Orthogonal Frequency Division Multiplexing
PA	Power Amplifier
PAE	Power Added Efficiency
PCB	Printed Circuit Board
PLE	Path Loss Exponent
QMH	Qualitative Microwave Holography
RAN	Radio Access Network

Abbreviation	Explanation
RAT	Radio Access Technology
RD	Relay Device
RF	Radio Frequency
RIS	Reconfigurable Intelligent Surface
RMSE	Root Mean Square Error
RS	Relay Station
Rx	Receiver
SAG	Selective-Area Growth
SC	Single Carrier
SiP	System-in-Package
SISO	Single-Input Single-Output
SIW	Substrate-Integrated Waveguide
SNR	Signal to Noise power Ratio
TDD	Time Division Duplex
TDS	Time Domain Spectroscopy
THz	Tera Hertz
TMA	Trimethylaluminum
TSV	Through-silicon Via
Tx	Transmitter
UCA	Uniform Circular Array
UE	User Equipment
UL	Up Link
VR	Virtual Reality